Receiver Site Optimisation for Passive Coherent Location (PCL) Radar System

Benson Chan

A project report submitted to the Department of Electrical Engineering,
University of Cape Town, in fulfilment of the requirements
for the degree of Bachelor of Science in Electrical Engineering.

Cape Town, October 2008

Declaration

I declare that this project report is my own, unaided work. All sources I have used or quoted have been indicated and acknowledged in the references. It is being submitted for the degree of Bachelor of Science in Electrical Engineering in the University of Cape Town. It has not been submitted before for any degree or examination in any other university.

Signature of Author .....

Cape Town

21 October 2008

Abstract

The Radar Remote Sensing Group in University of Cape Town has developed accurate modelling method that uses 3D maps of the Western Cape to predict the signal path loss between a transmitter, aircraft and a receiver in the Passive Coherent Location (PCL) system. The core objective of this thesis is to investigate the use of this modelling method to optimise the location of receivers in order to achieve maximum coverage of aircraft moving around Cape Town International Airport.

This project report investigates to approach the theory of Electro-magnetic (EM) propagation and EM simulations by using the available modelling tools. It has shown the coverage area only depends on the length of the baseline for desired SNR in a particular passive radar system. This report has also obtained theoretical formulation of the coverage area and a method to calculate the coverage area by using Matlab from the EM simulations for an one transmitter and one receiver passive radar.This will be followed by investigating on the problem with several receivers and one transmitter passive radar system.

Acknowledgements

First and foremost I would like to thank Professor Mike Inggs and Dr Yoann Paichard for their extremely helpful and patient supervision which enabled me to complete this project report. Secondly, I would like to thank Gunther Lange for his guidance and support. I would also like to thank my family and friends for their support throughout this period and lastly to the colleagues in the radar lab for their contributions.

Contents

List of Figures

List of Symbols

L	—	Baseline of the passive radar system
Tx	—	Transmitter
Rx	—	Receiver
C	—	Bistatic angle
α_T	—	Transmitter look angle
α_R	—	Receiver look angle
R_T	—	Transmitter-to-target range
R_R	—	Receiver-to-target range
P_T	—	Transmitted power
G_T	—	Gain of the transmitter's antenna
G_R	—	Gain of the receiver's antenna
λ	—	Wavelength
σ_B	—	Bistatic radar target cross section area (target RCS)
F_T	—	Transmitter pattern propagation factor
F_R	—	Receiver pattern propagation factor
k	—	Boltzman's constant
T_S	—	Receiver total noise temperature
B_n	—	Receiver noise bandwidth
$\left(\frac{S}{N}\right)_{min}$	—	Signal-to-noise ratio (SNR) needed for detection
L_T	—	Losses in transmitter
L_R	—	Losses in receiver
κ	—	Bistatic maximum range product
σ_M	—	Monostatic radar target cross section area (target RCS)
L_M	—	Target range for monostatic radar system
$F_T^{'}$	—	Transmitter propagation factor
$F_R^{'}$	—	Receiver propagation factor
f_T	—	Transmitter's antenna pattern factor
f_R	—	Receiver's antenna pattern factor
K	—	Bistatic radar constant

A	—	Amplitude of the sine wave
I_0	—	Modified Bessel function of zero order
Z	—	Argument
V_T	—	Threshold
P_d	—	Probability of detection
P_{fa}	—	Probability of a false alarm
ψ_0	—	Mean square value of the noise voltage
T_{fa}	—	False alarm time
B	—	IF bandwidth
A_{B1}	—	Coverage area for cosite region
A_{B2}	—	Coverage area for non-cosite region
A_C	—	Common coverage area
r_T	—	Radius of the transmitter's coverage area
r_R	—	Radius of the receiver's coverage area
h_t	—	Target altitude (km)
h_T	—	Altitude of the transmitter antenna (km)
h_R	—	Altitude of the receiver antenna (km)
c	—	Speed of light
f	—	Frequency
α	—	The angle between two baselines

Nomenclature

PCL—Passive Coherent Location

FM—Frequency modulated

AREPS—Advanced Refractive Effects Prediction System

APM—Advanced Propagation Model

CW—Continuous wave

OTH-B—Over-the-horizon-back-scatter

AOA—Angle of arrival

SNR—Signal-to-noise power ratio

RCS—Target cross section area

LOS—Light-of-sight

Azimuth—Angle in a horizontal plane, relative to a fixed reference, usually north or the longitudinal reference axis of the aircraft or satellite.

Beamwidth—The angular width of a slice through the mainlobe of the radiation pattern of an antenna in the horizontal, vertical or other plane.

Doppler frequency—A shift in the radio frequency of the return from a target or other object as a result of the object's radial motion relative to the radar.

Range—The radial distance from a radar to a target.

Chapter 1

Introduction

1.1 Background

The defining property of bistatic radar, is the transmitter and receiver are not co-located. This simply means the fact that the transmitter and receiver are not located at the same position in bistatic radar system. A Passive Coherent Location (PCL) system (also called Passive radar) is a special case of a bistatic radar and, more generally, multistatic radar, which is the case where the transmitters are non-cooperative [4].

Passive radars or Passive Coherent Location systems encompass a class of radar systems that detect and track objects by processing reception from non-cooperative sources of illumination in the environment, such as commercial broadcast systems such as television and radio and are commonly referred to as transmitters of opportunity.

PCL system does not contain transmitters (thus the term passive) but uses other emitters as transmitters [6], thus the achievable coverage depends not only on the transmitted power but also on the position of the receivers as well. Therefore, the optimisation of the receiver site becomes a very important issue in achieving maximum coverage in the passive radar system. This also emphasises the importance of receiver location information.

1.2 Objectives

The objectives of this thesis are:

- To investigate the use of the Advanced Refractive Effects Prediction System (AREPS) which developed by US Navy.
- To investigate the use of the Multistatic Radar Coverage Prediction Method which developed by Radar Remote Sensing Group in UCT (This method is based on the propagation loss data

which generated from AREPS).

- To investigate the relationship between coverage area and baseline (L)
- To validate the Multistatic Radar Coverage Prediction Method in the aspects of Oval of Cassini and coverage area with theoretical predictions which are based on theoretical equations.
- To minimise the intersection area for a one transmitter and two receivers case in order to achieve maximum area of coverage.
- To investigate the effects of terrain and multipath in the passive radar coverage.
- To optimise the location of passive radar receiver in order to achieve maximum coverage of aircraft moving around Cape Town International Airport.

These objectives are in essence quite broad, allowing for a variety of methods and techniques to be investigated and used. Yet, due to the broad nature of these objectives, the methods of the investigations and analyses in each chapter will be clearly stated.

1.3 Plan of Development

Chapter 1 forms the introduction to this thesis. The background to this topic is discussed and objectives of this project are presented here.

Chapter 2 is the literary review and presents various factors and information necessary and related to this thesis topic. The following topics will form the core to the literature review: The overview of the bistatic radar, including its definition, advantages & disadvantages and classification, is being discussed. This will be followed by a general description of passive radar. Within this description, brief history, typical illuminations and advantages & disadvantages of passive radar will be reviewed. Fundamental theories of bistatic radar, such as coordinate system, geometry, range relationship, probabilities of detection & false alarm and target coverage, will also be discussed. A brief description of APM & AREPS will be introduced. Finally, a Multistatic Radar Coverage Prediction Method which based on the interpolation of the propagation data from AREPS with Matlab presented by Gunther Lange will be discussed briefly at the end of this chapter.

Chapter 3 will introduce a detailed criterion of this project. A list of limitations and assumptions have been set-up before starting the investigation of this topic.

Chapter 4 The investigation of the relationship between SNR, baseline and coverage area, which based on the theoretical equations of bistatic radar, will be presented in this chapter. A mathematical

calculation for the maximum length of the baseline that will ensure the desired SNR falls within the cosite region in a given passive radar has been shown. Matlab will be used to plot and show the relationship between the baseline and coverage area.

Chapter 5 focuses on the coverage prediction without antenna gain involved in free space. The reason for limiting the theoretical coverage prediction without antenna gain involved and within the free space has been illustrated. This will be followed by the theoretical prediction of oval of Cassini and coverage area based on the theoretical equations. Matlab has been used to plot the theoretical oval of Cassini for SNR=15dB in our particular passive radar system. Thereafter, a Matlab script called FSArea.m has been created to calculate the approximated coverage area for a desired oval of Cassini, based on the SNR data generated from Multistatic Radar Coverage Prediction Method. A comparison between the theoretical prediction and simulated results have been made on the SNR coverage map and the coverage area.

The purpose of **Chapter 6** is to investigate of the effects of the antenna gain, multipath and terrain on the passive radar coverage. SNR coverage maps have been plotted by using Multistatic Radar Coverage Prediction Method. A Matlab script called OvalPlot_AREPS.m is used to plot the coverage area for the desired SNR (15dB), hence, coverage with these effects involved can be viewed visually.

Chapter 7 has been designed to investigate the coverage with the change in altitude. The altitude that being investigate is at 1600m. By using the Matlab script called FSArea.m, the approximated area can be calculated, and this value will be compared to the approximated area at 5000m. By comparing these two values of coverage, it verifies that the coverage will be less at low altitude as the effects of multipath and terrain will be lessened at high altitude.

Chapter 8 investigates the coverage area in an one transmitter and two receivers passive radar system. The method of tackling this problem has been discussed at the beginning of this chapter. The mathematical calculation used to achieve linear transformation and linear transformation with rotation of the axis in the polar coordinate, has also been shown. A Matlab script called OvalPlot_transfo_coordinate.m has been created to simulate and plot the area of intersection based on the expressions that have been shown in this chapter. The suggestion of finding the area of intersection for two ovals has also been provided.

Chapter 2

Literature Review

The following review of literature was done on subjects that relate to or affect the subject of the project undertaken. An overview of passive radar system will be outlined in the following few paragraphs. Bistatic radar fundamentals essential to the topic of the project will be discussed. AREPS and Multistatic Radar Coverage Prediction Method will also be introduced briefly at the end of this chapter.

2.1 Overview of Bistatic Radar

Bistatic radar is defined as a radar that uses antennas at different locations for transmission and reception. This means the fact that the transmitter and receiver are not co-located in the bistatic radar system. Recently, there are different versions of definition of bistatic radar as a conventional bistatic radar system does not specify how far the transmitting and receiving sites must be separated. Attempts have been made to quantify this separation by Skolnik and Blake. Both Blake's direction-distance and Skolnik's path separation criteria apply to all bistatic configuration. The purpose for establishing these separation criteria is simply to distinguish special types of radar, such as continuous wave (CW) and over-the-horizon-back-scatter (OTH-B) radars [11].

2.1.1 Advantages and Disadvantages of Bistatic Radar System

The principal advantages of Bistatic and Multistatic radar include [9]:

- Lower procurement and maintenance costs (if using a third party's transmitter, such as passive radar system)
- Operation without a frequency clearance (if using a third party's transmitter, such as passive radar system)

- Covert operation of the receiver
- Increased resilience to electronic countermeasure as waveform being used and receiver location are potentially unknown
- Possible enhanced radar cross section of the target due to geometrical effects

The principal disadvantages of bistatic and multistatic radar include:

- System complexity
- Costs of providing communication between sites
- Lack of control over transmitter (if exploiting a third party transmitter)
- Harder to deploy
- Reduced low-level coverage due to the need for line-of-sight from several locations

2.1.2 Specific Classes of Bistatic Radar

Generally, there are four specific classes of bistatic radar. These four specific classes include [9]:

1. **Pseudo-monostatic radar** has the angle which subtended between transmitter, target and receiver (the bistatic angle) is close to zero.
2. **Forward scatter radar** is the bistatic radar that be designed to operate in a fence-like configuration, detecting targets which pass between the transmitter and receiver, with the bistatic angle near 180 degrees.
3. **Multistatic radar** is one in which there are at least three components - for example, one receiver and two transmitter, or two receivers and one transmitter, or multiple receivers and multiple transmitters. It is a generalisation of the bistatic radar system, with one or more receivers processing returns from one or more geographically separated transmitters.
4. **Passive radar** is a bistatic or multistatic radar that exploits non-radar transmitters of opportunity. This radar system is also known as Passive Coherent Location (PCL) system. Passive radar is the specific type of the bistatic radar that being investigated in this project.

2.2 Overview of Passive Radar

A passive radar is a special case of a bistatic radar [4].In a passive radar system, there is no dedicated transmitter. Instead, the receiver uses third-party transmitters in the environment, and measures the time difference of arrival between the signal arriving directly from the transmitter and the signal arriving via reflection from the object. So, the bistatic range of the object can be calculated. In addition to bistatic range, a passive radar will typically also measure the bistatic Doppler shift of the echo and also its direction of arrival. Therefore, the location, heading and speed of the object can be calculated. Multiple transmitters and/or receivers will be introduced to make different independent measurements in order to improve the final track accuracy and the area of coverage [10].

2.2.1 Brief History of Passive Radar

The concept of passive radar detection - using reflected ambient radio signals emanating from a distant transmitter - is not now. The first radar experiments in the United Kingdom in 1935 by Robert Watson - Watt demonstrated the principle of radar by detecting a Handley Page Heyford bomber at a distance of 12 km Using the BBC shortwave transmitter at Daventry.

Early radars were all bistatic because the technology to enable an antenna to be switched from transmit to receiver mode had not been developed. Thus many countries were using bistatic systems in air defence network during the early 1930s.

The Germans used a passive bistatic system during World War II. This system, call the Kleine Heidelberg device, was located at Ostend and operated as a bistatic receiver, using the British Chain Home radars as non-cooperative illuminators, to detect aircraft over the southern part of North Sea.

Bistatic radar systems gave way to monostatic systems with the development of the synchronizer in 1936 since the monostatic systems were much easier to implement. In the early 1950s, bistatic systems were considered again when some interesting properties of the scattered radar energy were discovered, indeed the term “bistatic” was first used by Seigel in 1955 in his report describing these properties.

Experiments in the United States led to the deployment of a bistatic system in North American Distant Early Warning Line around 1955.

The rise of cheap computing power and digital receiver technology in the 1980s led to a resurgence of interest in passive radar technology. For the first time, these allowed designers to apply digital signal processing techniques to exploit a variety of broadcast signals and to use cross-correlation techniques to achieve sufficient signal processing gain to detect targets and estimated their bistatic range and Doppler shift. Classified programmes existed in several nations, but the first announcement of a commercial system was by Lockheed-Martin Mission Systems in 1998, with the commercial launch of the Silent Sentru system, that exploited FM radio and analogue television transmitters [10].

2.2.2 Typical Illumination of Passive Radar

Passive radar systems have been developed the exploit the following sources of illumination [10]:

- Analog television signals
- FM radio signals
- GSM base stations
- Digital audio broadcasting
- Digital video broadcasting
- Terrestrial High-definition television transmitters in North America

Satellite signals have generally been found to be inadequate for passive radar use: either because the powers are too low, or because the orbits of the satellites are such that illumination is too infrequent.

2.2.3 Advantages and Disadvantages of Passive Radar System

The advantages of passive radar system over conventional bistatic radar system are [10]:

- Physically small and hence easily deployed in places where conventional radars cannot be
- Capabilities against stealth aircraft due to the frequency bands and multistatic geometries employed
- Rapid updated, typically once a second
- Difficulty of jamming
- Resilience to anti-radiation missiles

The disadvantages of passive radar system over conventional bistatic radar system are [10]:

- Immaturity
- Reliance on third-party illuminators
- Complexity of deployment
- 2D operation

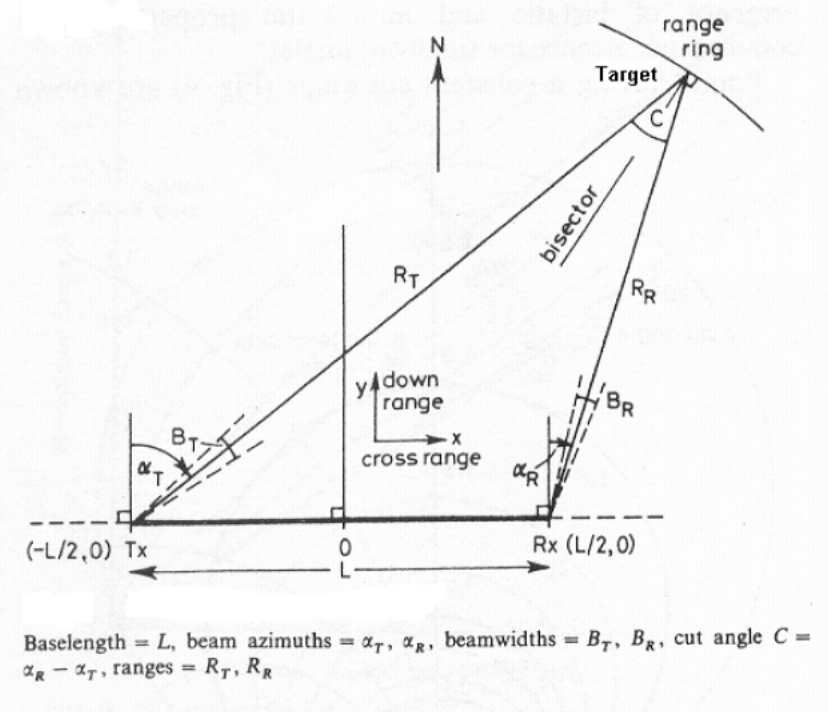

Baselength = L, beam azimuths = α_T, α_R, beamwidths = B_T, B_R, cut angle $C = \alpha_R - \alpha_T$, ranges = R_T, R_R

Figure 2.1: Geometry of a bistatic radar, North-referenced coordinate system in two dimensions. [11]

2.3 Coordinate Systems and Geometry

Due to the separate positioning locations of the transmitter and the receiver, the coordinate system and the geometry of a bistatic radar system can be complex in a way.

The coordinate system used to describe the geometry will be in a two dimensional case, a north referenced coordinate system which shown on Figure 2.1. The bistatic plane, is the plane on which the transmitter (Tx), receiver (Rx) and the target (on the edge of the range ring) lie. On this particular plane, the ellipse with its foci at Tx and Rx is also presented (the range ring). This ellipse has its midpoint located on the midpoint of the transmitter and receiver stations.

All the ellipses have a common transmitting and receiving site foci, and therefore a common baseline (L). The bistatic system which is shown in Figure 2.1, is known as the bistatic triangle.

As shown on the Figure 2.1, the baseline (L) is the distance between the transmitter (Tx) and receiver (Rx). The distance from the transmitter to the target is defined as RT and from the receiver to the target is RR.

The bistatic angle is C, or β, which is also known as the cut angle, which is the angle between the transmitter and the receiver, with the vertex at the target. The transmitter look angle is α_T and the receiver look angle is α_R. Counter clockwise direction will be taken as positive for the look angles. They are also known as the angle of arrival (AOA) [11]. Also, note that:

$$\alpha_T + \alpha_R = C = \beta \tag{2.1}$$

In a general case, the bistatic system works the same, irrespective of whether the target lies above or below the baseline. This is due to its symmetrical nature of their geometry.

2.4 Range Relationships

The bistatic range equation is similar in form to the monostatic range equation and is derived in a similar process. The effect of the propagation factors on the range will be mentioned briefly and the ovals of Cassini (SNR contours) will also be discussed in detail later in this section.

2.4.1 Bistatic Radar Range Equations

The range equations for a bistatic radar are derived in a manner that exactly the same way in the monostatic radar case. The derivation of these equations can be found in [7]. With this analog, the bistatic radar maximum range equation, from Willis [11], is shown below.

$$(R_T R_R)_{max} = \left[\frac{P_T G_T G_R \lambda^2 \sigma_B F_T^2 F_R^2}{(4\pi)^3 k T_s B_n \left(\frac{S}{N}\right)_{min} L_T L_R} \right]^{\frac{1}{2}} \tag{2.2}$$

or

$$(R_T R_R)_{max} = \kappa \tag{2.3}$$

where

R_T = transmitter-to-target range

R_R = receiver-to-target range

P_T = transmitted power

G_T = gain of the transmitter's antenna

G_R = gain of the receiver's antenna

λ = wavelength

σ_B = bistatic radar target cross section area (target RCS)

F_T = transmitter pattern propagation factor

F_R= receiver pattern propagation factor

k = Boltzman's constant

T_S= receiver total noise temperature

B_n= receiver noise bandwidth

$\left(\frac{S}{N}\right)_{min}$ = signal-to-noise ratio (SNR) needed for detection

L_T = losses in transmitter (cables, signal processing, etc.)

L_R = losses in receiver (cables, signal processing, etc.)

κ = bistatic maximum range product

The FM radio broadcast antenna is assumed to be omni-directional, and therefore 0dBi gain can be assumed. Also, for calculation purposes, we first assume the pattern propagation factor $F_R = F_T = 1$. For this bistatic radar maximum range equation to be reduced to monostatic case, the following variables needs to be changed [11]:

1. $\sigma_B = \sigma_M$
2. $L_T L_R = L_M$
3. $R_T^2 R_R^2 = (R_T R_R)^2 = \left(R_M^2\right)^2 = R_M^4$

Note that $(R_M)_{max} = \sqrt{\kappa}$. The term $\sqrt{\kappa}$ is sometimes called the equivalent monostatic range, which occurs when the transmitting and receiving sites are located at the same location [5].

2.4.2 Pattern Propagation Factors

The transmitting and receiving pattern propagation factors, F_T and F_R, are the product of the propagation factor ($F_T^{'}$ and $F_R^{'}$) and antenna pattern factor (f_T and f_R) respectively. The pattern propagation factors take into account the gains of the transmit and receive antennas as a pointing angle. The losses in the signal (atmospheric, absorption, etc) are also taken into account while propagating through the atmosphere. More about the pattern propagation factors can be found in [11].

2.4.3 Ovals of Cassini

The formal definition of an oval of Cassini is the locus of the vertex of a triangle when the product of the sides adjacent to the vertex is constant and the length of the opposite side is fixed [3]. In the bistatic radar system, the oval of Cassini is defined as the SNR contours, whereby the product of the range from transmitter and receiver to the target (R_T and R_R respectively), the range product ($R_T R_R$), is kept constant for each contour. In order to obtain these contours, the radar range equation in Section 2.4.1 is needed to be solved for the SNR, which will give us:

$$S/N = \frac{P_T G_T G_R \lambda^2 \sigma_B F_T^2 F_R^2}{(4\pi)^3 k T_s B_n L_T L_R R_T^2 R_R^2} \tag{2.4}$$

or

$$S/N = \frac{K}{R_T^2 R_R^2} \tag{2.5}$$

where S/N is the signal-to-noise power ratio at the range R_T and R_R, and

$$K = \frac{P_T G_T G_R \lambda^2 \sigma_B F_T^2 F_R^2}{(4\pi)^3 k T_s B_n L_T L_R} \tag{2.6}$$

The term K is called the bistatic radar constant, and is related to the bistatic maximum range product κ and minimum SNR value. Therefore, the minimum SNR contour can be obtained from the Equation 2.5.

$$\left(\frac{S}{N}\right)_{min} = \frac{K}{\kappa^2} \tag{2.7}$$

A convenient way to plot ovals of Cassini is in a polar coordinate (r, θ) system. The geometry of this polar coordinate system is shown in Figure 2.2 below.

Converting R_T and R_R into polar coordinates gives [11]:

$$R_T^2 R_R^2 = \left(r^2 + \frac{L^2}{4}\right)^2 - r^2 L^2 \cos^2\theta \tag{2.8}$$

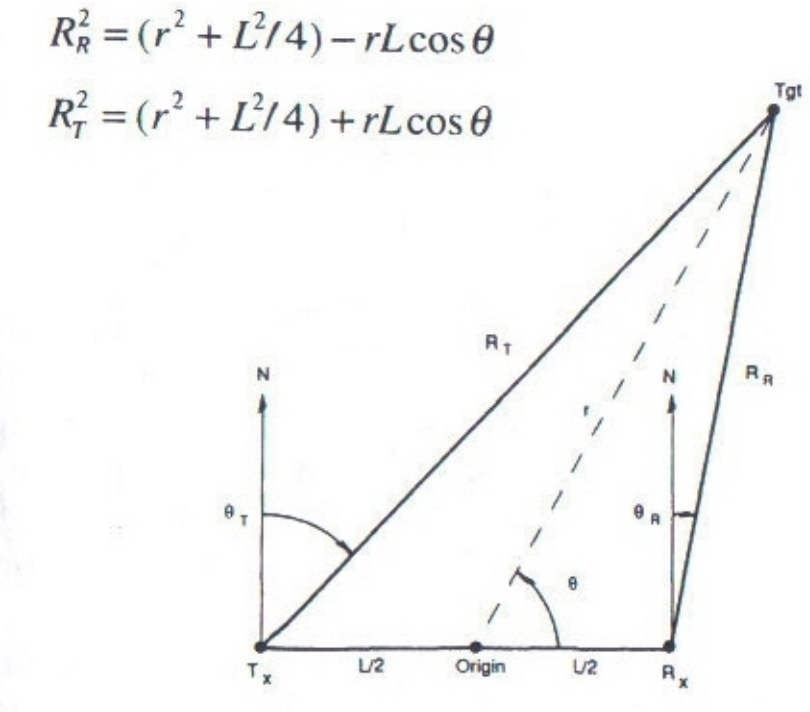

Figure 2.2: Geometry for converting North-referenced coordinates into polar coordinates (r, θ). [11]

Substituting Equation 2.8 into Equation 2.5 gives:

$$S/N = \frac{K}{\left(r^2 + \frac{L^2}{4}\right)^2 - r^2 L^2 \cos^2\theta} \tag{2.9}$$

These ovals of Cassini (signal-to-noise ratio contours) for $10dB \leq \frac{S}{N} \leq 30dB$, can be seen in Figure 2.3 below.

As shown on the Figure 2.3, the oval shrinks and finally collapses around the transmitter and receiver as the SNR increases. This same effect occurs as the baseline is increased. The mid-point on the baseline where the oval breaks into two parts is called the *cusp*. The oval is called a lemniscate (of two parts) at this S/N . At this point, $r = 0$, and from the SNR equation 2.9which shown above, we got [11]:

$$S/N = 16K/L^4 \tag{2.10}$$

Assuming that $(S/N) = (S/N)_{min}$ for this lemniscate, yields [11]

$$L = 2\sqrt{\kappa} \tag{2.11}$$

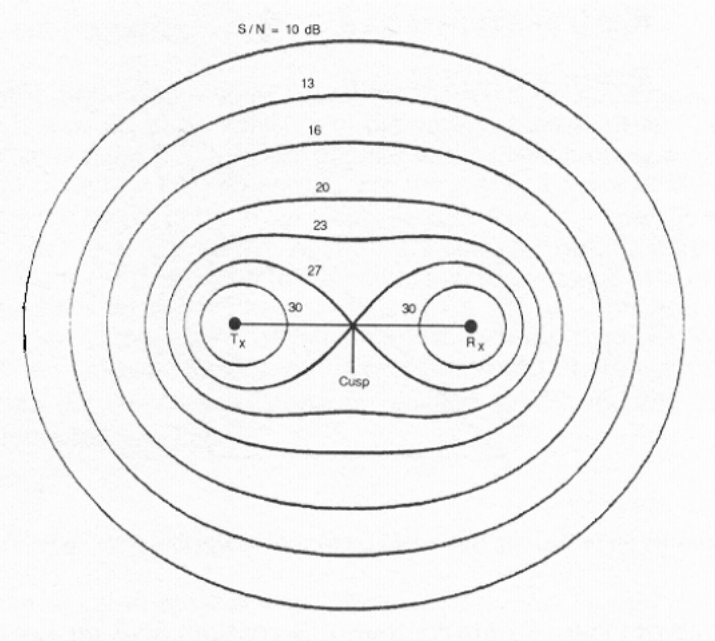

Figure 2.3: Contours of a constant SNR - ovals of Cassini. [11]

2.4.4 Operating Regions

From the equations in Section 2.4.3, three main operating regions can be defined [11], namely:

1. **The receiver centred region** - occurs when $L > 2\sqrt{\kappa}$ and $R_T \gg R_R$, hence the oval breaks into two parts.

2. **The transmitter centred region** - occurs when $L > 2\sqrt{\kappa}$ and $R_T \ll R_R$, hence the oval breaks into two parts.

3. **The cosite region** - occurs when $L < 2\sqrt{\kappa}$, therefore the oval remains single (oval does not develop a *cusp* or break into two parts, refer to Figure 2.3).

2.5 Probabilities of Detection and False Alarm

A specific probability of detection and probability of false alarm is required to achieve minimum signal-to-noise ratio ($\left(\frac{S}{N}\right)_{min}$, shown in Section 2.4.1 and 2.4.3). From Equation 2.7 above, the minimum signal-to-noise ratio is needed in order to calculate the bistatic maximum range product (κ) for a given bistatic constant,K [8], i.e.: given basic information of the specific bistatic radar system such as the transmitted power and gain of transmitter's & receiver's antenna, etc (see Equation 2.6 for details).

2.5.1 Probability of Detection

Now, let's consider an echo signal represented as a sinewave of amplitude A along with Gaussian noise at the input of the envelope detector. The probability density function of the envelope R at the video output is given by Rice probability density function,

$$p_s(R) = \frac{R}{\psi_0} \exp\left(-\frac{R^2 + A^2}{2\psi_0}\right) I_0\left(\frac{RA}{\psi_0}\right) \tag{2.12}$$

where I_0 is the modified Bessel function of zero order and argument Z. The probability of detecting the signal is the probability that the envelop R will exceed the threshold V_T (set by the need to achieve some specific false-alarm time). Thus the probability of detection is

$$P_d = \int_{V_T}^{\infty} p_s(R)\, dR \tag{2.13}$$

A series approximation method will be used to solve for P_d after substituting the Equation 2.12 into Equation 2.13. Numerical and empirical methods can also be used [8]. The expression of the probability of detection $P_d$in terms of SNR can be seen in [8]. Hence, the relationship between the probability of detection and SNR & probability of false alarm can be shown in the Figure 3.1 in Chapter 3.1.

2.5.2 Probability of False Alarm

The probability of a false alarm, P_{fa}, is denoted as

$$P_{fa} = \exp\left(-\frac{-V_T^2}{2\psi_0}\right) \tag{2.14}$$

where $V_T$is the voltage threshold and ψ_0 is the mean square value of the noise voltage (mean noise power).

or

$$P_{fa} = \frac{1}{T_{fa}B} \tag{2.15}$$

where T_{fa} is the false alarm time and B is the IF bandwidth.

The detailed derivation of the probability of false alarm equation can be seen in [8]. The false-alarm probabilities of radars are generally quite small since a decision as to whether a target is present or not is made every $1/B$ second. The bandwidth B is usually large, so there are many opportunities during one second for a false alarm to occur. If the threshold is set slightly higher than required and maintained stable, there is little likelihood of false alarms due to thermal noise. In practice, false

alarms are more likely to occur from clutter echoes (ground, sea, weather, birds, and insects) that enter the radar and are large enough to cross the threshold [8].

2.6 Target Coverage

Coverage is an important factor in bistatic radars, and this can be defined as the area on the bistatic plane whereby the target is visible to both the transmitter and receiver. Bistatic coverage is detected in two ways [11]:

1. **Detection-constrained coverage.** This type of coverage is constrained by the maximum range product of the oval of Cassini $(R_T R_R)_{max}$. When the oval of Cassini encapsulates both the transmitter and the receiver (the cosite region), the coverage area can be approximated by:

$$A_{B1} \approx \pi\kappa \left\{ 1 - \left(\frac{1}{64}\right)\left(\frac{L^4}{\kappa^2}\right) - \left(\frac{3}{16384}\right)\left(\frac{L^8}{\kappa^4}\right) \right\} \tag{2.16}$$

   But when the oval of Cassini surrounds the transmitter and receiver with two separate circles, the coverage area is approximated by:

$$A_{B2} \approx \left(\frac{2\pi\kappa^2}{L^2}\right)\left(1 + \frac{2\kappa^2}{L^4} + \frac{12\kappa^4}{L^8} + \frac{100\kappa^6}{L^{12}}\right) \tag{2.17}$$

   In a monostatic case (i.e.: transmitter and receiver locate at the same position), therefore, L = 0, and the coverage area for the monostatic radar becomes:

$$A_M = \pi\kappa = \pi\,(R_M)^2_{max} \tag{2.18}$$

   this is expected, as the oval becomes circular in shape in the monostatic radar system. In Figure 2.4 below, it is shown how the coverage area of bistatic radar A_B varies with respect to the monostatic area A_M, as a function of the normalised baseline range, $L/\sqrt{\kappa}$. It is assumed that a suitable LOS exists between transmitter, target and receiver [11].

2. **Line-of-sight constrained coverage.** For any given target, transmitter, and receiver altitudes, the target must be in the LOS of both the transmitter and receiver sites. For a flat earth, these requirements are established by coverage circles centred at each site. Targets in the area which common to both circles, A_C, have a LOS to both transmitter and receiver sites as shown in Figure 2.5 [11].

   This coverage area shown in Figure 2.5 is the effective radar horizon coverage area for a smooth earth model, as shown from the equations to follow. In usual circumstances, the coverage area is affected by multipath, refraction, diffraction, shadowing and earth curvature. For

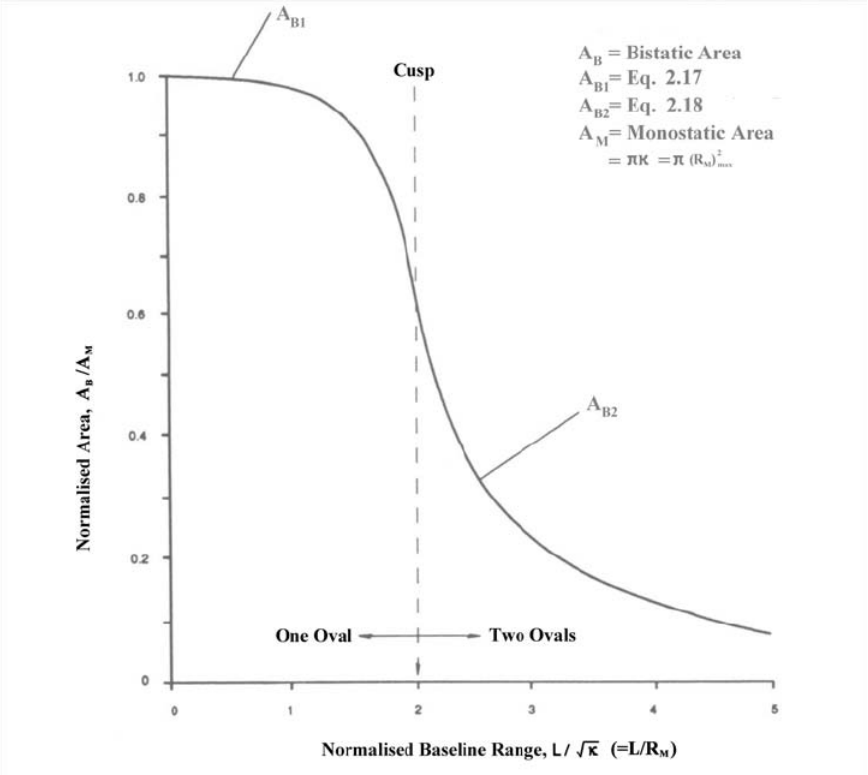

Figure 2.4: Ratio of bistatic area (oval of Cassini) to monostatic area. [11]

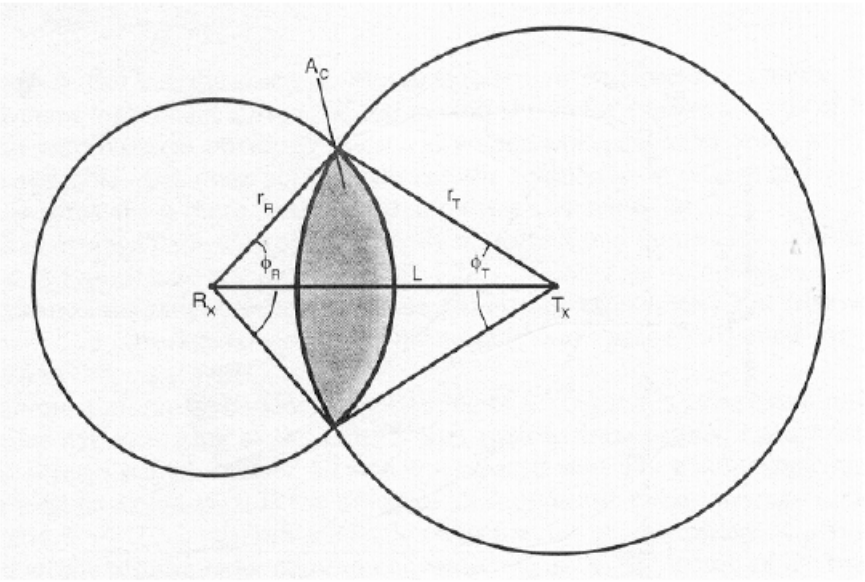

Figure 2.5: Geometry of a common coverage area, A_C. [11]

a $\frac{4}{3}$ earth model, and ignoring multipath lobing, the radius of the coverage areas can be approximated in kilometres by the following equations [11].

$$r_T \propto 130\left(\sqrt{\sqrt{h_t}+\sqrt{h_T}}\right) \tag{2.19}$$

$$r_R \propto 130\left(\sqrt{\sqrt{h_t}+\sqrt{h_R}}\right) \tag{2.20}$$

where
r_T = radius of the transmitter's coverage area
r_R = radius of the receiver's coverage area
h_t = target altitude (km)
h_T = altitude of the transmitter antenna (km)
h_R = altitude of the receiver antenna (km)
These derivation of these equations can be found in Willis [11]. The common area between the transmitter and the receiver is the intersection area between the two circles.

$$A_C = \frac{1}{2}\left[r_R^2\left(\phi_R - \sin\phi_R\right) + r_T^2\left(\phi_T - \sin\phi_T\right)\right] \tag{2.21}$$

where
$\phi_R = 2\arccos\left(\frac{r_R^2 - r_T^2 + L^2}{2r_R L}\right)$
$\phi_T = 2\arccos\left(\frac{r_T^2 - r_R^2 + L^2}{2r_T L}\right)$
These equations are valid for $L + r_R > r_T > L - r_R$ or $L + r_T > r_R > L - r_T$. Whenever the right-hand side of either inequality is not satisfied such that $r_T + r_R \leq L$ then $A_C = 0$. This means that the coverage areas of the transmitter and receiver do not intersect. When the left-hand side of the first inequality, $A_C = \pi r_T^2$. This is because the receiver's coverage includes the transmitter's coverage completely, and vice-versa.

For our particular system, the detection-constrainted coverage method will be used to investigate the coverage of our specific passive radar system. Our coverages area is also mainly dependent on our antenna system, i.e.: the information of transmitter and receiver, can be seen in Chapter 3.3.

2.7 Advanced Propagation Model and AREPS

Advanced Refractive Effects Prediction System, is also called AREPS, which was developed in 2003 by the Space and Naval Warfare Systems centre of US Navy at San Diego [2]. The Advanced Propagation Model (APM) is the propagation model used within AREPS [1]. APM is a hybrid ray optics and parabolic equation propagation model, functional for all frequencies between 2MHz and

57GHz. The advantageous feature of the APM and AREPS software is the propagation factor, F, can be computed from them, given relevant regional terrain and atmospheric data.

The goal in the development of APM was to create an all-encompassing propagation model for the incorporation into the U.S. military's electromagnetic performance assessment systems. In addition to its use by the U.S. military and other U.S. government agencies, APM and AREPS are well-proven and widely used by academic institutions and foreign agencies across the world [4].

2.8 Multistatic Radar Coverage Prediction Method

Multistatic Radar Coverage Prediction Method, also called MRCPM in this report, is an accurate modelling method that developed by the Radar Remote Sensing Group in University of Cape Town. It uses the propagation loss data generated by APM and captured from AREPS, to predict the signal path loss among a transmitter, aircraft & a receiver and spatial coverage in the Passive Coherent Location (PCL) system. The coverage plots which generated from this method, are in the form of spatial signal-to-noise ratio (SNR) maps. These SNR maps can provide a visual means for determining the radar detection range and coverage feasibility. The details of this prediction method can be seen in [4]. The best advantage of this method is the propagation loss data in a specific passive radar system which generated from AREPS, is converted into SNR data by this method. According to the relationship between the SNR, maximum range product (κ) and coverage area shown in previous sections, hence, it provides us a powerful tool to investigate the detection range and the optimisation of coverage in passive radar system.

Chapter 3

Project Criterion Setup

As the scope of the topic of this project is very broad, therefore, it is necessary to setup a set of criterion throughout the whole project execution. The detailed criterion setup for this project will be discussed in this chapter.

3.1 Signal-to-noise ratio setup

Albersheim developed a simple empirical formula for the relationship between signal-to-noise ratio ($\frac{S}{N}$), probability of detection (P_d) and probability of false alarm (P_{fa}), which is

$$S/N = A + 0.12AB + 1.7B \tag{3.1}$$

where

$$A = ln\left[0.62/P_{fa}\right] \text{ and } B = ln\left[P_d/(1-P_d)\right]$$

Note that, the signal-to-noise ratio in the above equation is numerical, and not in dB; and ln is the natural logarithm [8]. From the Equation 3.1 above, it shows the SNR depends on the values of the probability of detection and false alarm. For the passive radar system that investigated in this project, supposes that the average time between false alarms is required to be 1.5 min, i.e.:T_{fa}= 1.5min. And the bandwidth of the IF is 100kHz, i.e.:B=100kHz. From the Equation 2.15, the probability of false alarm can be obtained.

$$P_{fa} = \frac{1}{T_{fa}B} = \frac{1}{(1.5\times 60)\,(100\times 10^3)} \approx 1.11\times 10^{-7}$$

The relationship between SNR, P_{fa} and P_d can be shown in the Figure 3.1. This relationship figure shows for probability of false alarm equals to 1×10^{-7}, signal-to-noise ratio of 12dB is required for a probability of detection of 0.50, 15dB for $P_d = 0.99$, and 15.75dB for $P_d = 0.998$. Thus, a change

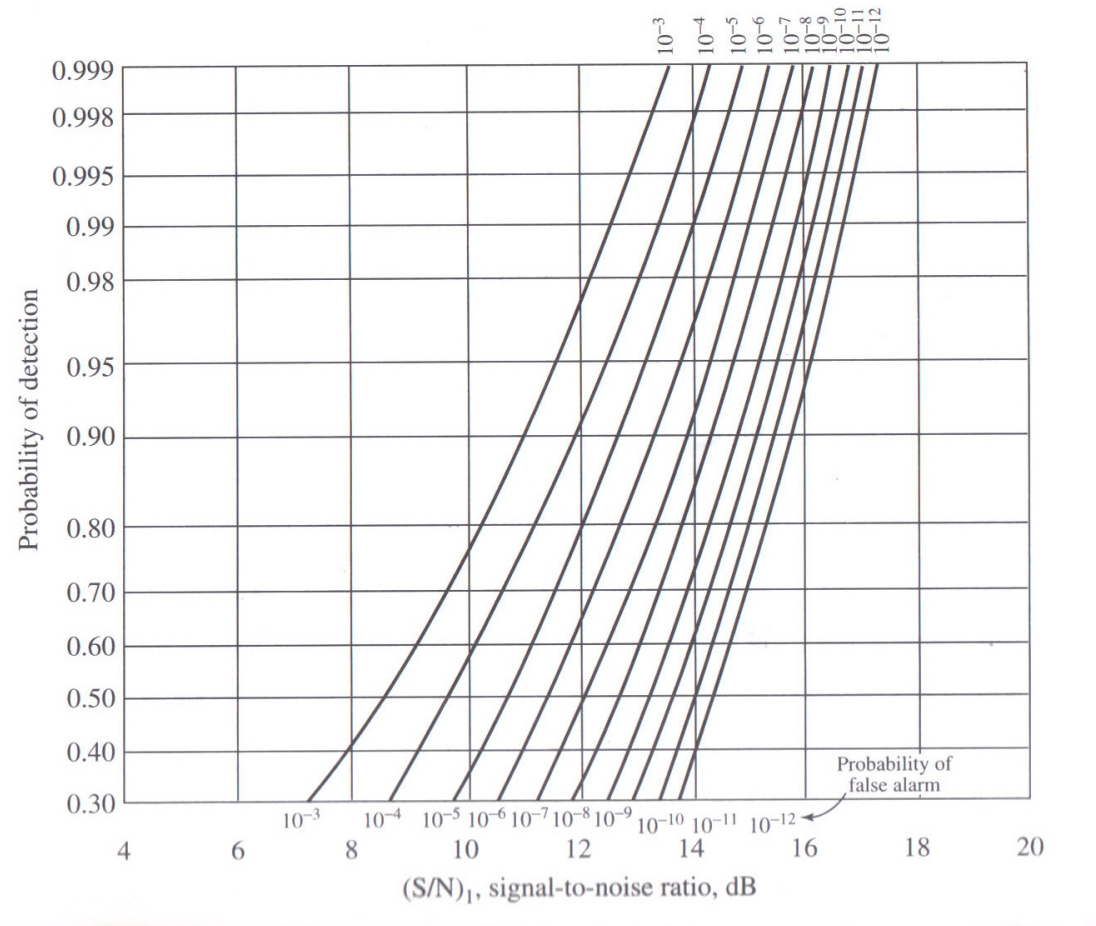

Figure 3.1: Probability of detection as a function of the signal-to-noise (power) ratio and the probability of false alarm. [8]

of 3dB can mean the difference between highly reliable detection (0.99) and marginal detection (0.5). This probability of false alarm curve has a significant change of probability of detection between SNR of 11dB and 15dB. However, as the SNR increased more than 15dB, the probability of detection will only change very slightly as the increasing of the SNR, as shown in Figure 3.1. Also, a probability of detection of 0.99 can be considered as a highly reliable detection. Therefore, $SNR = 15dB$ has been set as our desired (interesting) signal-to-noise ratio in our investigated radar system.

3.2 Altitude and Coverage Range Setup

The target altitude that is to be investigated is 5000m, as it is the standard height for an airport approach. For avoiding the complexity, the transmitter and receiver can be assumed to be of the same altitude. The reason for assuming this case is shown as following: for instance, if the LOS distance between the transmitter and receiver is 120km, and their height difference is 60m. So, according to the Pythagorean theorem, the actual distance (surface distance) between the transmitter and receiver will be: $B = \sqrt{C^2 - A^2} = \sqrt{(120 \times 10^3)^2 - 60^2} \approx 119.999km$. The surface distance is almost same as the direct LOS distance, as the length of hypotenuse is much longer than the length of leg. Therefore, we can assume Tx and Rx are at the same altitude.

The range of investigation will cover all the area within 150km radius from the airport. The distance between transmitter and receiver (baseline length, L) will be limited within 150km in this project. The reason for setting up this criterion will be discussed in next chapter.

3.3 Passive Radar System Setup

In this project, specific transmitter and receiver have been chosen in order to conduct a better investigation on the coverage in the passive radar system practically. The chosen transmitter is Villiersdorp transmitter and the chosen receiver is Menzies receiver. The detailed information of the chosen transmitter and receiver is shown below:

[Transmitter information]

1. Tx Name = Villiersdorp
2. Tx Latitude [d,m,s,Hemi] = 33,58,9,S
3. Tx Longitude [d,m,s,Hemi] = 19,30,25,E
4. AREPS Tx Project Folder Name = VilliersdorpTx96.5
5. Frequency [MHz] = 96.5

6. Power [W] = 1000
7. Beamwidth start [0-359 deg] = 0
8. Beamwidth end [0-359 deg] = 359
9. Gain within beamwidth [dB] = 10
10. Gain outside beamwidth [dB] = -30

[Receiver Information]

1. Rx Name = Menzies
2. Rx Latitude [d,m,s,Hemi] = 33,57,31.16,S
3. Rx Longitude [d,m,s,Hemi] = 18,27,36.36,E
4. AREPS Rx Project Folder Name = MenziesRx96.5
5. Antenna Pattern [data file] = AntPat.mat
6. Rx Beamwidth start [0-359 deg] = 0
7. Rx Beamwidth end [0-359 deg] = 359
8. Pad receiver beamwidth [y/n] = n
9. Padded beamwidth [deg] = 5
10. Receiver Noise Figure Fn [dB] = 10

In addition, the surface distance between Villiersdorp transmitter and Menzies receiver is $L = 96.53km$. The explanation of specific transmitter and receiver has to be chosen before investigation of passive radar coverage is shown in the Chapter 3.4.

3.4 Bistatic Constant Setup

A bistatic constant, K, must be given in order to investigate the coverage area for a specific SNR in a passive radar system. Equations 2.16 and 2.17 shows the there is significant link between the coverage area and the maximum range product κ. Also, the Equation 2.7 can be written as

$$\kappa^2 = \frac{K}{\left(\frac{S}{N}\right)_{min}} \tag{3.2}$$

or

$$\kappa = \sqrt{\frac{K}{\left(\frac{S}{N}\right)_{min}}} \tag{3.3}$$

For a given SNR, we need to specify the value of bistatic constant, K, to obtain the value for maximum range product,κ. Therefore, bistatic constant (K) must be specified in order to calculate the coverage area for a given SNR theoretically. Note that, from the bistatic constant equation shown in Equation 2.6, the bistatic constant depends on the specified information from the transmitter and receiver. Different passive radar system or different combinations of transmitter and receiver will result in different values of bistatic constant (K). This is the reason why transmitter and receiver needs to be specified before starting to investigate passive radar coverage.

From the information shown in Chapter 3.3, the bistatic constant (K) without antenna gain can be obtained.

$$K = \frac{1000 \times 1 \times 1 \times \left(\frac{3000}{965}\right)^2 \times 10 \times 1^2 \times 1^2}{(4\pi)^3 \times 1.38 \times 10^{-23} \times 2900 \times 1 \times 1 \times 1} \approx 1.217 \times 10^{21}$$

Note that:

For a bistatic constant without antenna gain involves, $G_T = G_R = 1$. Wave length $\lambda = \frac{c}{f} = \frac{3\times10^8 m/s}{96.5\times10^6 Hz} = \frac{3000}{965}m$. The transmitter and receiver pattern propagation factor, $F_T = F_R = 1$. The losses in transmitter and receiver, $L_T = L_R = 1$. The target cross section area is set to be $10m^2$. The receiver noise bandwidth in the equation which is the same as the SNR processing bandwidth as shown in the information above. The total receiver noise temperature can be obtained from $T_s = T_0 + T_e = T_0 + (F-1) \times T_0 = 290 + (10-1) \times 290 = 2900K$.

Chapter 4

Investigation of The Relationship Between SNR, Baseline and Coverage Area

4.1 Relationship Between SNR and Baseline

As mentioned in Chapter 3.1, signal-to-noise ratio of 15dB is the desired SNR in this project. From Equation 2.10 which shown in Chapter 2.4.3, it shows the SNR equation for the oval of Cassini just breaks into two parts. This project will only interest the oval of Cassini which does not develop a *cusp*. Therefore, for a given SNR, the maximum range of the baseline (L) which will not result the oval break into two parts, can be found from the Equation 2.10.

$$L = \left(\frac{16K}{S/N}\right)^{1/4} \approx 511km$$

As specified in Chapter 3.2, the baseline for our system is limited to within 150km, which is much smaller than the maximum range of the baseline shown above, 511km. Therefore, it will make sure that the oval of Cassini (SNR contour) of $SNR = 15dB$ will never break into two parts in our passive radar system.

4.2 Relationship Between Coverage Area and Baseline

According to the Equation 3.3, bistatic maximum range product, κ, can be obtained from a given passive radar system (K given) and SNR. A Matlab script called Area_vs_Baseline_Plot.m has been created to plot and show different values of the coverage area for baseline (L) varies from 0 to 150km based on the Equation 2.16. This plot is shown in Figure 4.1.

Figure 4.1 shows the value of coverage area decreases as the length of baseline increases. Also, the curve only decreases gently from 0 to 100km, but starts decreasing dramatically from 100km

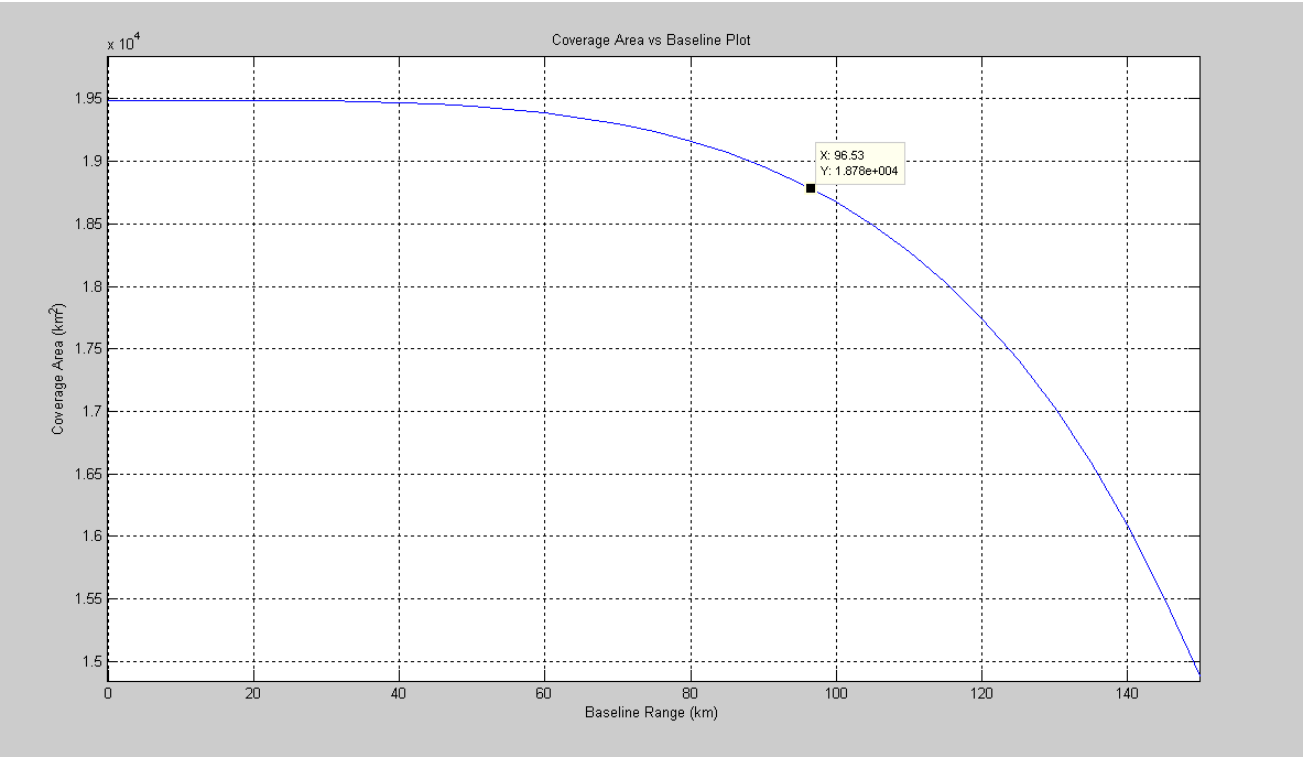

Figure 4.1: Relationship between coverage area and baseline (L)

to 150km and keeps decreasing further as the baseline (L) increases. Therefore, the best distance between transmitter and receiver should be from 0-100km in order to achieve more coverage in a passive radar system. The investigated system in this project has a baseline of 96.53km which also falls into the above desired region. And it has a predicted coverage area of $1.878 \times 10^4 km^2$ shown in the Figure 4.1. The theoretical calculation of the coverage area will be shown in detail later in this project.

In conclusion, Equation 3.3 tells us the bistatic maximum range product, κ, will be a constant value for a given passive radar system (i.e.: Kgiven) and desired SNR. Therefore, the area of coverage in a given passive radar system only depends on baseline (L) for a specific desired SNR (signal-to-noise ratio of 15dB will be the case in this project).

Chapter 5

Coverage Prediction Without Antenna Gain Involved in Free Space

A free-space theoretical prediction can carried out easily in a specific passive radar system. However, it will be very difficult to predict the oval of Cassini of $SNR = 15dB$ and coverage area with antenna gain, terrain and multipath effects involved theoretically. For instance, take the passive radar system which is being investigated in this project as an example to illustrate the difficulty of the theoretical prediction that has antenna gain, terrain and multipath effects involved. A Matlab script called gain_vs_phase_plot.m has been made to plot the gain pattern of the receiver's antenna, which is shown in Figure 5.1.

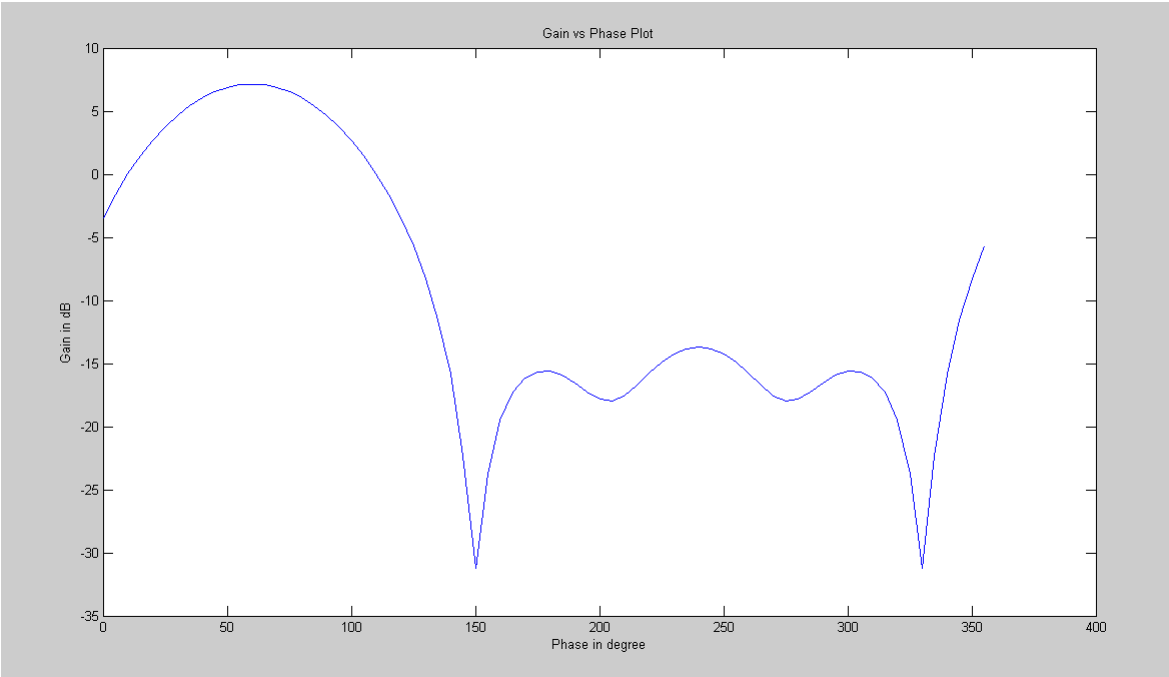

Figure 5.1: Plot of Gain vs Phase of the receiver's antenna

Figure 5.1 shows the gain of receiver's antenna changes as the phase changes. The gain of receiver (G_R) is not a constant value but a function of the phase. Hence, the value of the bistatic constant (K) will also change with the change of receiver gain (G_R) according to the bistatic constant equation. Therefore, it is difficult to predict the theoretical coverage area with the antenna gain involved. The effects of terrain and multipath will result in change of the value of transmitter & receiver pattern propagation factors (F_T & F_R) in the bistatic constant equation, hence, results in changes of the bistatic constant value. This is the reason why theoretical prediction is very difficult to be achieved with terrain and multipath effects involved.

5.1 Theoretical Prediction of Oval of Cassini and Coverage Area

An investigation has been done on predicting the oval of Cassini and Coverage Area of our specific system theoretically. Rewriting the equation shown in 2.9:

$$\left(r^2+\frac{L^2}{4}\right)^2-r^2L^2\cos^2\theta=C\,(constant) \tag{5.1}$$

or

$$r^4+r^2\left(\frac{1}{2}L^2-L^2\cos^2\theta\right)+\left(\frac{L^4}{16}-C\right)=0 \tag{5.2}$$

where

$$C=\frac{K}{S/N}=\frac{1.217\times10^{21}}{10^{\frac{15}{10}}}\approx3.848\times10^{19}$$

By letting $x=r^2$, Equation 5.2 becomes:

$$x^2+x\left(\frac{1}{2}L^2-L^2\cos^2\theta\right)+\left(\frac{L^4}{16}-C\right)=0 \tag{5.3}$$

Therefore, x can be solved in terms of θonly as the length of the baseline is known ($L=96.53km$) from the formulae $x=\frac{-b\pm\sqrt{b^2-4ac}}{2a}$. Due to $x=r^2$, x must be ≥ 0 and r is the radius distance from the centre to point on the curve, so r will also be a value ≥ 0. So, there is only one solution for r for one specific phase angle (θ). A script called OvalPlot.m has been created with Matlab to plot the predicted oval of Cassini for our system in polar coordinate based on Equation 5.3. The figure of the predicted oval of Cassini in polar coordinate can be seen in Figure 5.2.

According to the Equation 2.16 and 3.3, the theoretical prediction of the coverage area of our passive radar system will be obtained as follows:

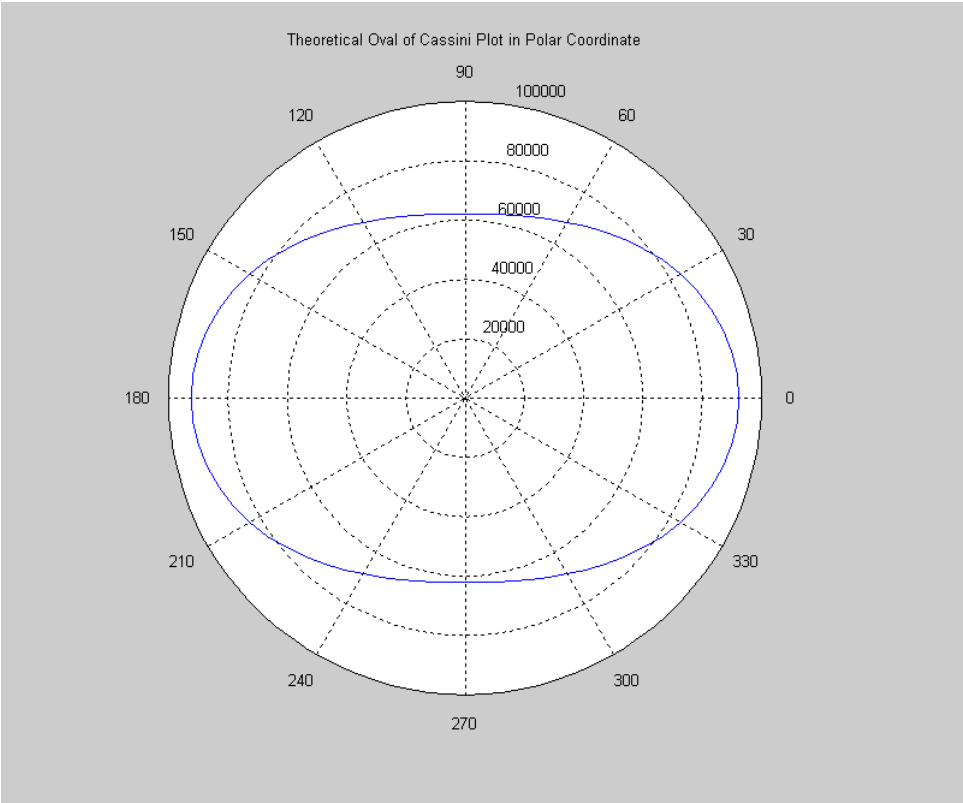

Figure 5.2: Theoretical oval of Cassini plot in polar coordinate for SNR=15dB

$$A = \pi \times 6.204 \times 10^9 \left\{ \left(1 - \frac{1}{64}\right) \left(\frac{\left(9.653 \times 10^4\right)^4}{\left(6.204 \times 10^9\right)^2} \right) - \left(\frac{3}{16384} \right) \left(\frac{\left(9.653 \times 10^4\right)^8}{\left(6.204 \times 10^9\right)^4} \right) \right\} \approx 1.8784 \times 10^4 km^2$$

where

$$L = 9.653 \times 10^4 m \text{ and } \kappa = \sqrt{\frac{K}{S/N}} \approx 6.204 \times 10^9$$

5.2 Verification of The Theoretical Prediction

In this section, AREPS, MRCPM and a Matlab script called FSArea.m has been used to simulate the SNR coverage map and to integrate the area for desired signal-to-ratio, in order to verify them with the theoretical prediction that has been done in Chapter 5.1.

5.2.1 Oval of Cassini Verification by using AREPS & MRCPM

As mentioned in Chapter 2.7 and 2.8, the Multistatic Radar Coverage Prediction Method (MRCPM) is a method to plot the SNR coverage maps based on an interpolation of propagation loss data

generated by the Advanced Propagation Model (APM) and captured from the Advanced Refractive Effects Prediction System (AREPS). A SNR coverage map has been created for our system at 5000m altitude in free space by using this method, shown in Figure 5.3.

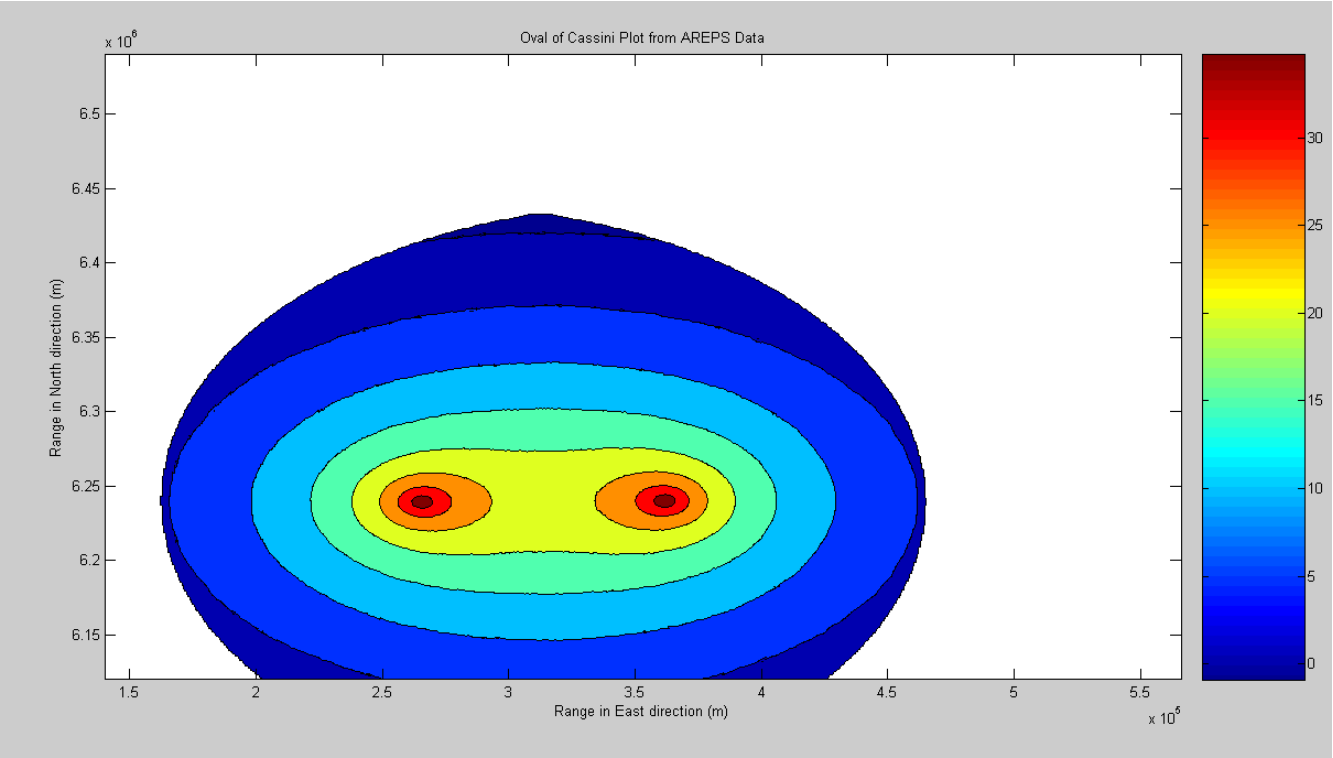

Figure 5.3: SNR coverage contours at 5000m altitude in free space without antenna gain involved

Figure 5.3 looks very similar to the theoretical SNR coverage map shown in Figure 2.3 in Chapter 2.4.3. This is expected, as they both show the SNR coverage contours in free space in a particular bistatic radar system. The colour bar at the right hand side indicates the values of the SNR (in dB) for different ovals of Cassini. The SNR value is getting larger and larger as it gets close to the centre of the oval, and at around 25dB, the oval of Cassini breaks into two parts completely. This also verifies the simulation from AREPS and MRCPM is consistent with the theoretical equation and prediction.

5.2.2 Coverage Area Verification

A script called FSArea.m has been made to plot the coverage area for the desired SNR (15dB), and to calculate the approximated value of the desired area by integrating all interested cell areas from the simulation data. This script will firstly take the SNR data generated from the Multistatic Radar Coverage Prediction Method, then set all the SNR that bigger than 15dB to be 1, otherwise be 0. Therefore, the coverage area of desired SNR can be plot, shown in Figure 5.4, by using a Matlab script called OvalPlot_AREPS.m.

The area in red shown in Figure 5.4 is the coverage area for our desired SNR (15dB). It is a oval

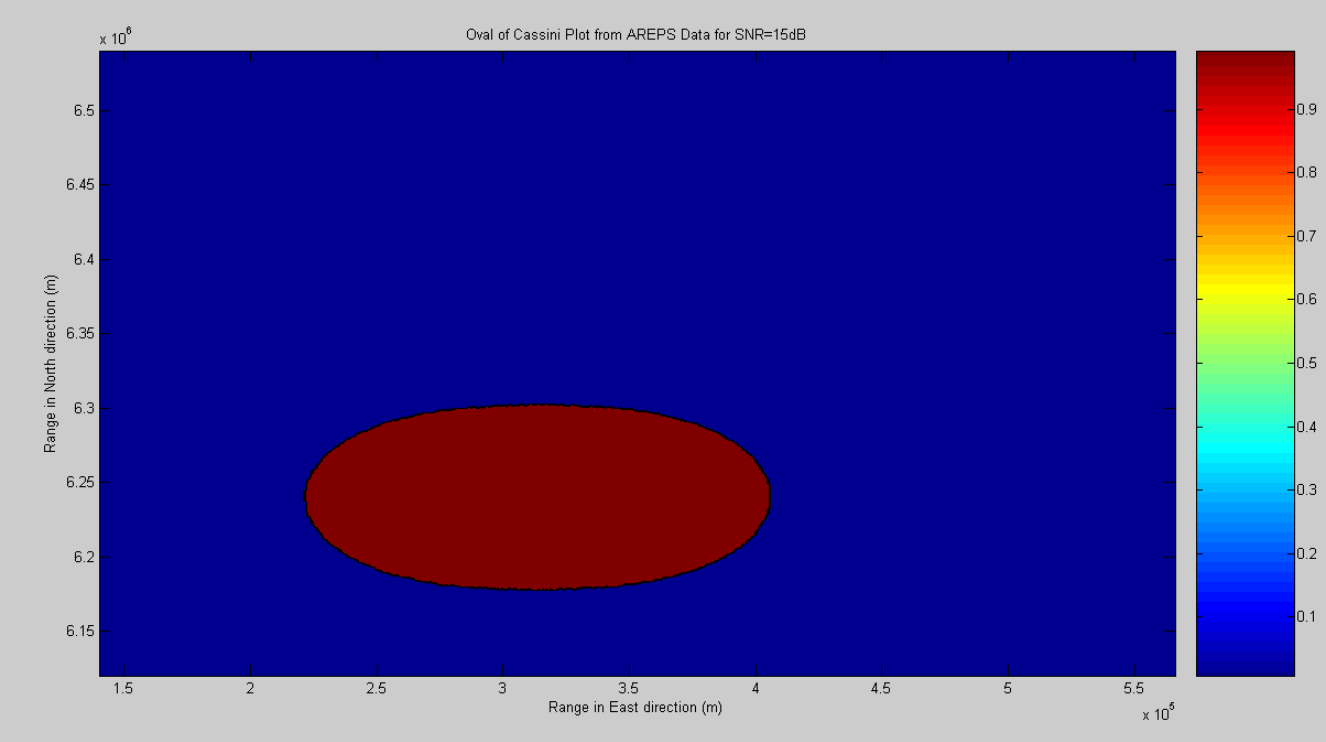

Figure 5.4: Oval of Cassini plot for SNR=15dB at 5000m altitude in free space without antenna gain involved

shape in free space, which is expected, as within this oval, the maximum range product (κ) remains constant. The SNR data is obtained from the uniform sampling of data, sampling will be made every 600 meters in east and north direction. Therefore, we can imagine the desired area is formed by combining many cubic blocks, each has a area of $600m \times 600m = 0.36km^2$. Therefore, an approximation of area can be made by counting up the total numbers of '1's in the desired area and multiplying it with the constant area for each cell ($0.36km^2$). This is exactly what the FSArea.m file does, and it returns an approximated area of $1.8692 \times 10^4 km^2$.

The area obtained from FSArea.m is slight different from the theoretical prediction, $1.8784 \times 10^4 km^2$. It has an error of:

$$error = \frac{A_{approximated} - A_{predicted}}{A_{predicted}} = \frac{1.8692 \times 10^4 km^2 - 1.8784 \times 10^4 km^2}{1.8784 \times 10^4 km^2} \approx -0.4898\%$$

This error can be neglected as its absolute value is less than 0.5%. Therefore, it proved that the function FSArea.m is correct, as it returns an approximated area that is consistent with the area calculated from the theoretical equation shown in Equation 2.16.

In addition, the reason for the slight difference between the integrated area value and predicted value is that the amount of samples that have been taken are not large enough. As the number of samples increases, the accuracy of calculated coverage area will tend to the real coverage area.

Chapter 6

Investigation of the Coverage with Antenna Gain, Terrain and Multipath Effects Involved

As discussed at the beginning of Chapter 5, it is difficult to predict the coverage with antenna gain, terrain and multipath effects involved theoretically. So, the coverage prediction with these effects will be carried out by using the AREPS, Multistatic Radar Coverage Prediction Method and the FSArea.m Matlab script in this chapter.

6.1 SNR and Area Coverage with Antenna Gain in free space

The SNR coverage maps that will be shown in this section for the cases that with antenna gain involved in free space and not in free space (i.e.: with terrain and multipath effects involved).

Figure 6.1 shows the SNR coverage map with antenna gain in free space. The signal-to-noise-ratio map looks similar to the antenna gain pattern and with significant high SNR value at the direction of the main-lobe propagation, but low small SNR value at the side-lobe region. This is expected, as the receiver gain pattern figure(Figure 5.1) shows the antenna gain of the receiver only focus on a particular phase region ($50^o - 70^o$).

This type of coverage is actually useful in the application of the aircraft's detection. This is due to the fact that each aircraft takes off or lands at the airport will have a set route. Therefore, aircrafts will be active in a particular direction from the airport; by using this coverage method, the passive radar system can focus on the direction that aircrafts moving toward and away the airport, to improve the probability of detection and save energy on the receiver's antenna.

Now, the SNR data with antenna gain involved, which generated from Multistatic Radar Coverage Prediction Method, has been interpolated into OvalPlot_AREPS.m and FSArea.m to plot the cover-

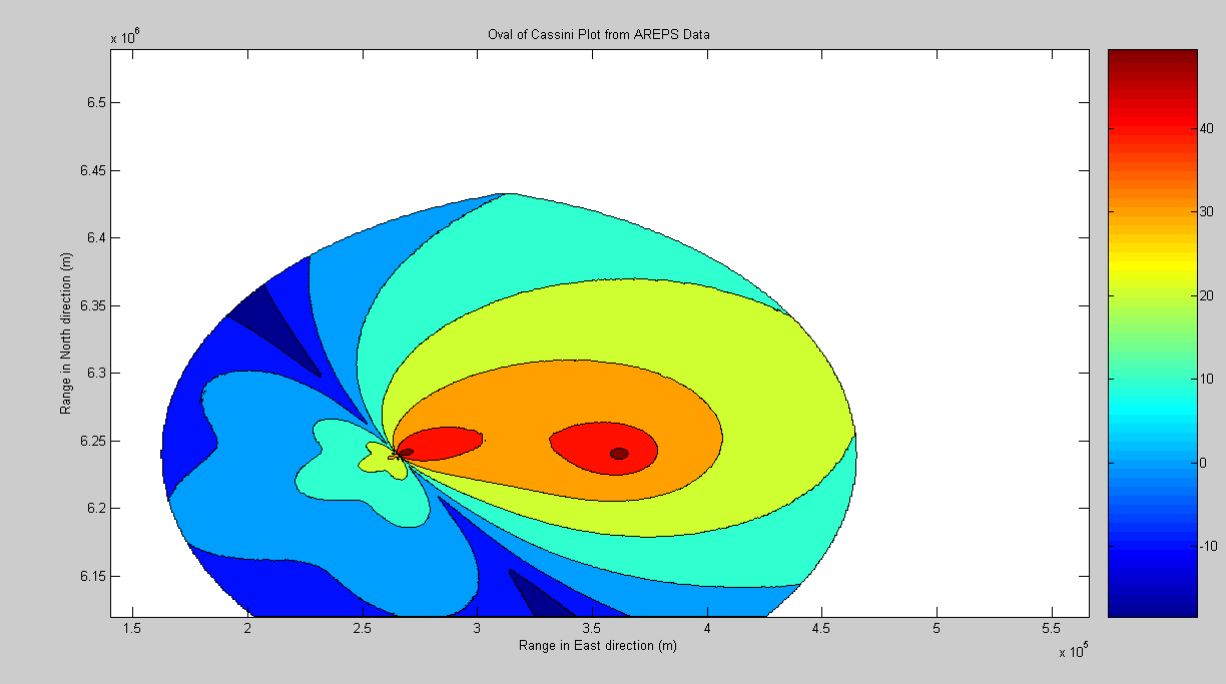

Figure 6.1: SNR coverage contours at 5000m altitude in free space with antenna gain involved

age area for SNR=15dB (shown in Figure 6.2) and to calculate its approximated area. The returned approximated area is $4.027 \times 10^4 km^2$.

6.2 SNR and Area Coverage with Antenna Gain and Multipath Effects due to The Flat Ground

Generally, the radar tracks a target aircraft via two paths. One is the direct path from radar to target and the other path includes a reflection from earth's surface. Also, the effects of multipath depend on what part of the antenna pattern strikes the surface [8]. Figure 6.3 shows the effects of multipath due to the flat ground on the SNR coverage map. By comparing the Figures 6.1 and 6.3, noting that the multipath effects due to the flat ground cause the SNR contours change in shape. The shape becomes irrational compared to it in free space.

Looking at Figure 6.3 and 6.1, it is evident that the simulated predicted coverage is less compared to the conventional case which is in free space. The reduction is not unexpected, yet it is important to note the significant effect that multipath, diffraction, refration and other atmospheric and terrain effects have on the bistatic SNR radar equation and radar detection range.

The SNR data with multipath and terrain effects is interpolated into Matlab scripts called OvalPlot_AREPS.m and FSArea.m. The coverage area for SNR=15dB can be obtained, as shown in Figure 6.4. The approximated area is $4.1121 \times 10^4 km^2$.

There have been a number of methods demonstrated or proposed for reducing multipath effects, such

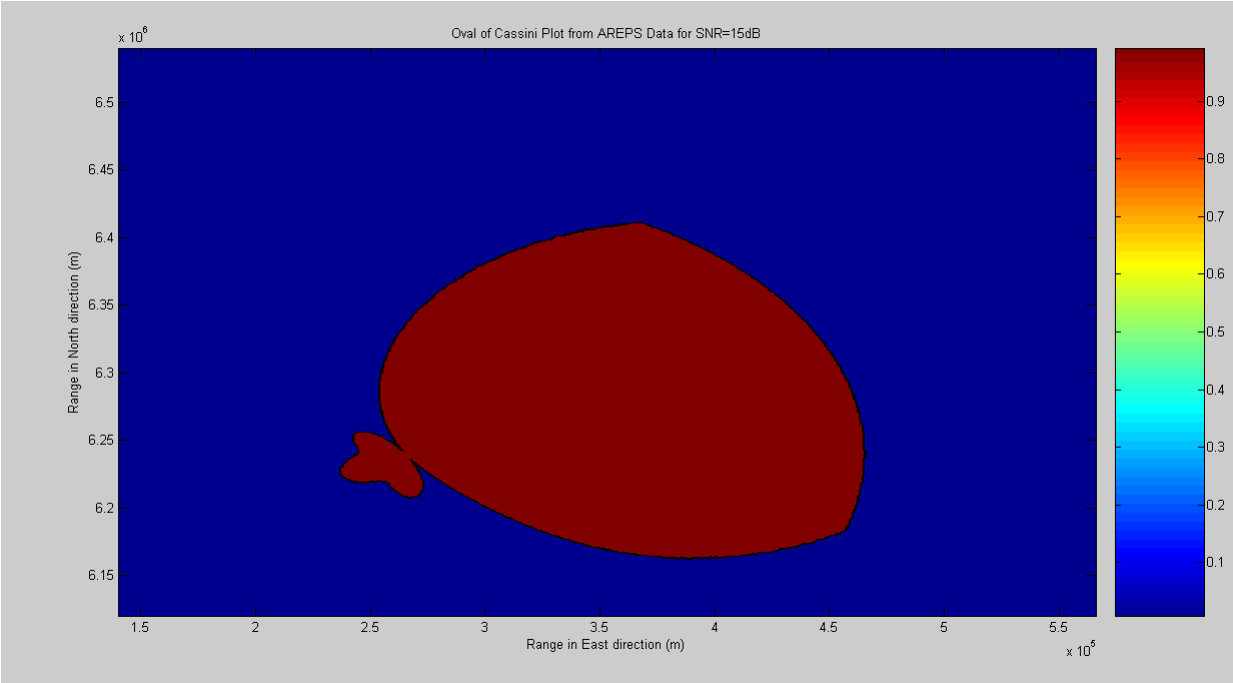

Figure 6.2: Oval of Cassini plot for SNR=15dB at 5000m altitude in free space with antenna gain involved

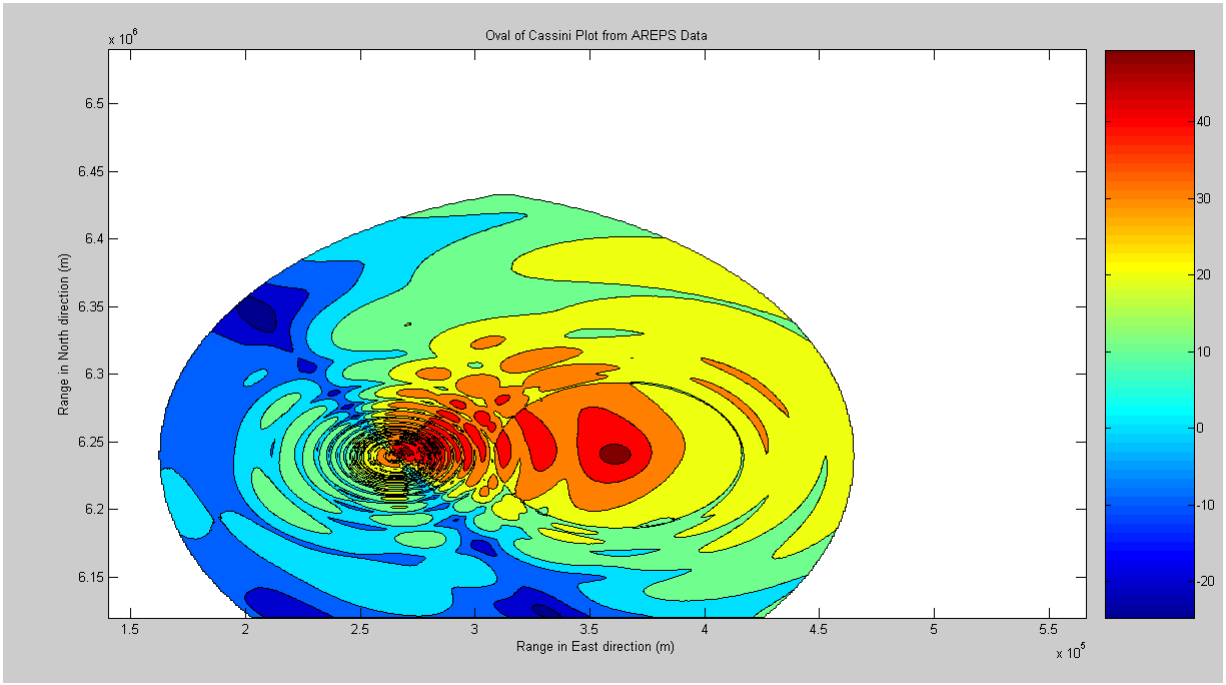

Figure 6.3: SNR coverage contours at 5000m altitude with antenna gain and multipath effects due to the flat ground

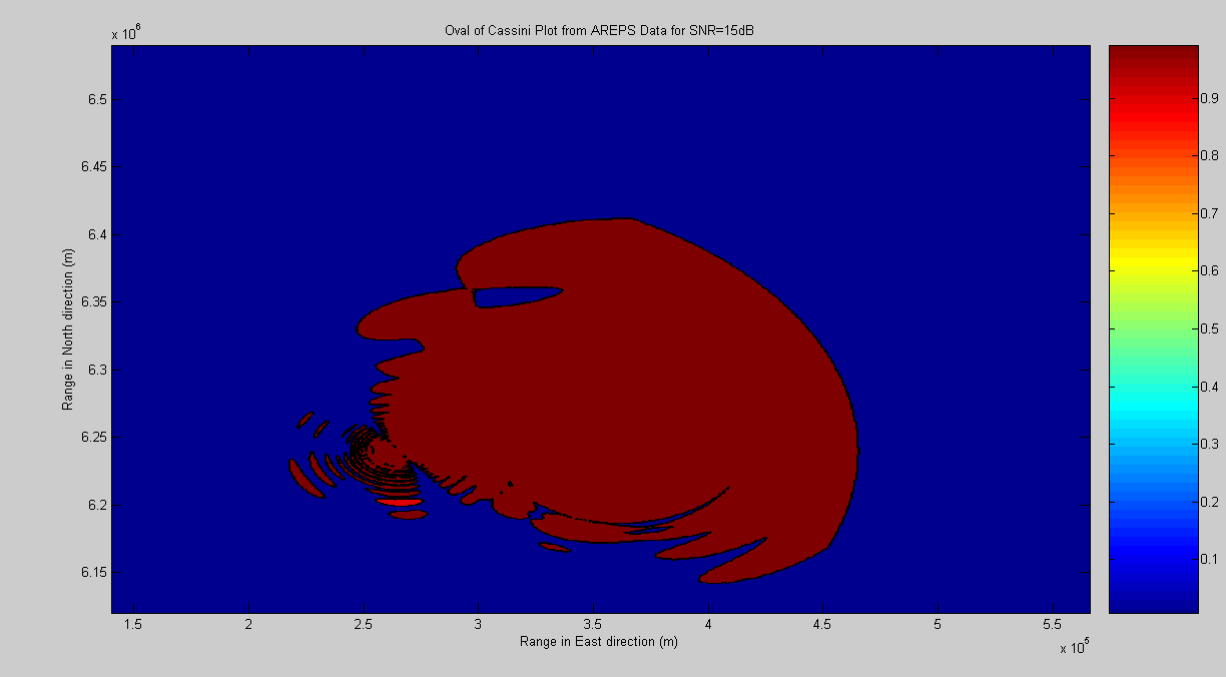

Figure 6.4: Oval of Cassini plot for SNR=15dB at 5000m altitude with antenna gain and multipath effects due to the flat ground

as Illogical Target Trajectory, Frequency Agility and Double-Null Elevation-Difference Pattern, etc. The details can be seen in [8].

Chapter 7

Investigation of Coverage with Different Altitude

An altitude of 5000m has been assumed in the previous chapters. Now, the effects of the change in altitude on coverage area are going to be investigated in this chapter. In this chapter, an altitude of 1600m has been chosen as the investigated altitude.

The Multistatic Radar Coverage Prediction Method has been used to extract the propagation loss data at the altitude of 1600m from AREPS and transform these propagation loss data into SNR data. The SNR coverage map with the multipath effects due to the flat ground has been shown in Figure 7.1.

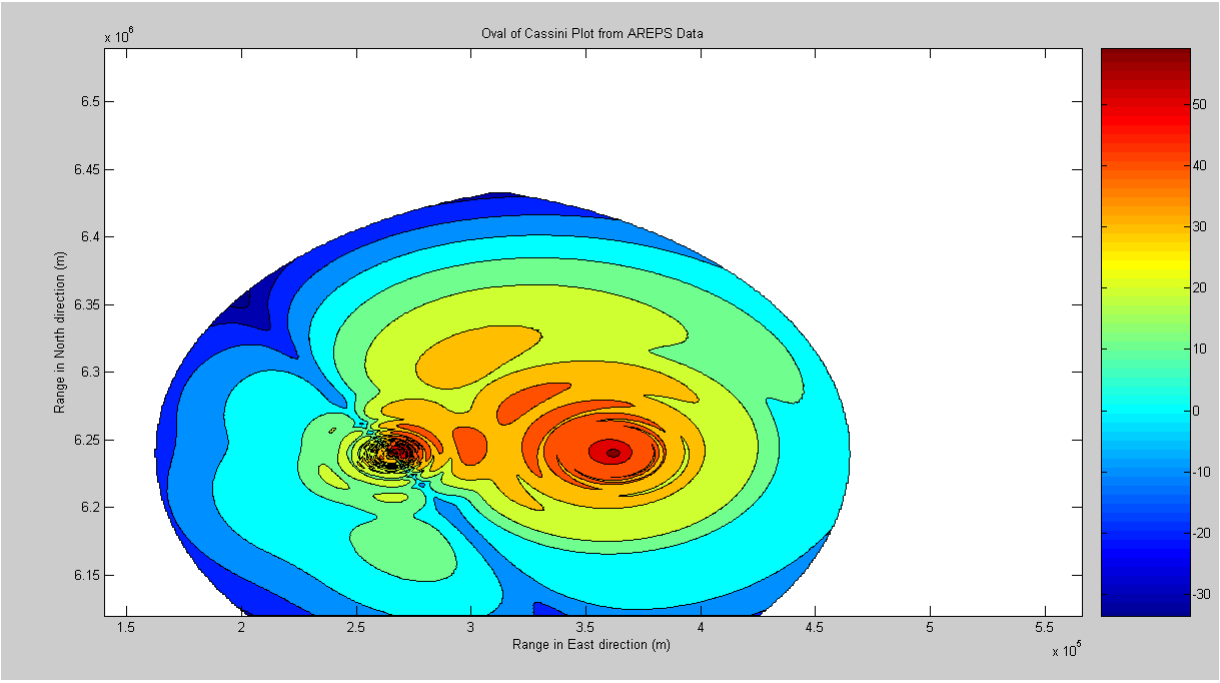

Figure 7.1: SNR coverage contours at 1600m altitude with antenna gain and multipath effects due to the flat ground

Figure 7.1 illustrates the simulated prediction coverage for an altitude of 1600m. By comparing this figure with Figure 6.3 which for an altitude of 5000m, this figure is expected because there is worse coverage at lower altitudes. At lower altitudes the effects of the multipath and terrain on the propagation factor have strengthened. Consequently, a close correlation between Figure 7.1 and Figure 6.3 becomes apparent as the AREPS generated propagation loss tends towards free-space propagation loss at high altitude.

Again, the SNR data at 1600m altitude is interpolated into Matlab scripts called OvalPlot_AREPS.m and FSArea.m. Hence, the coverage area for SNR=15dB can be obtained, as shown in Figure 7.2. The approximated area is $3.0486 \times 10^4 km^2$, this is much smaller than $4.1121 \times 10^4 km^2$, which is the area for altitude at 5000m, shown in Chapter 6.2. This verifies the fact that the coverage area will be smaller at lower altitude.

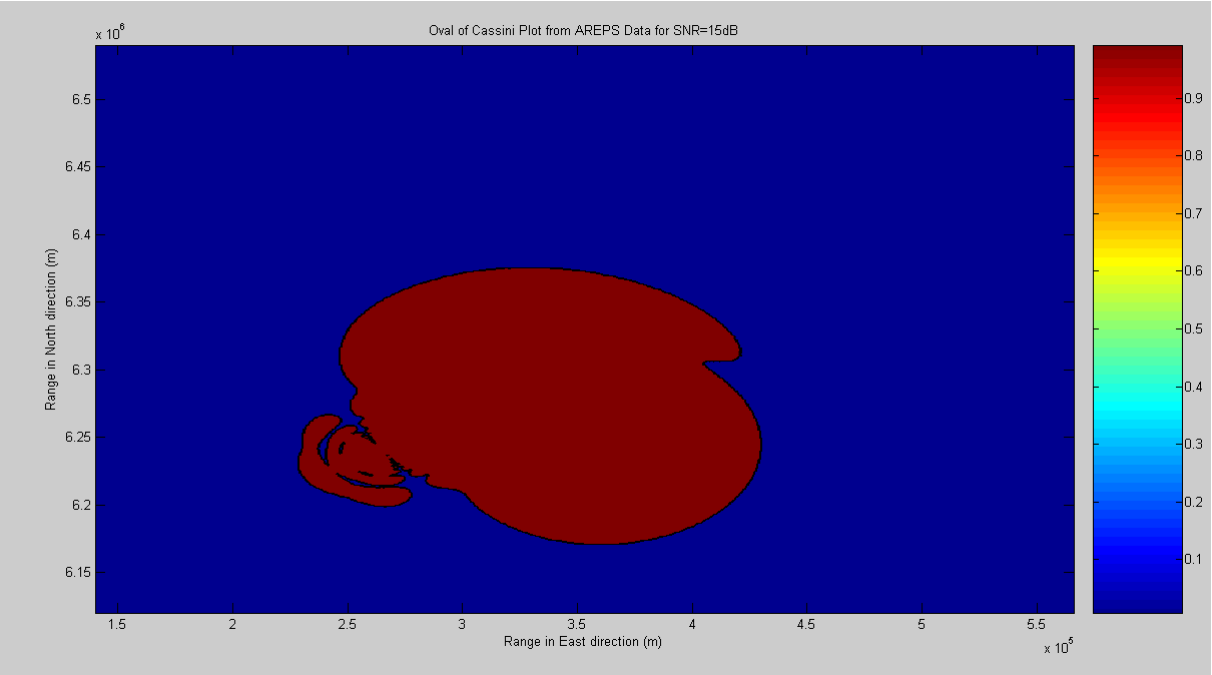

Figure 7.2: Oval of Cassini plot for SNR=15dB at 1600m altitude with antenna gain and multipath effects due to the flat ground

Chapter 8

Investigation of Coverage for An One Transmitter & Two Receivers Passive Radar System

The coverage for one transmitter and one receiver passive radar system has been analysed in Chapter 3 to Chapter 7. A two transmitters and one receiver passive radar system is going to be investigated in this chapter.

8.1 Problem Discussion

The coverage in an one transmitter and two receivers radar system is much more complicate than in the system that contains one transmitter and one receiver, hence, the problem will firstly be tackled from a mathematical prospective. Figure 8.1 shows the standard coverage for the one transmitter & two receivers passive radar system, where A represents the coverage area for desired SNR in T_X & R_{X1} system, B represents the coverage area for particular SNR in T_X & R_{X1} system and C (shaded region) is the area of intersection between area A and area B.

As shown in Figure 8.1, the total coverage area for this system is equal to the sum of the area of two ovals of Cassini, then subtract the area of intersection, also can be shown as following:

$$Area = A + B - C \tag{8.1}$$

Equations 2.16 and 3.3 tell us that the values of parameters A and B will be constant for a desired SNR in a particular passive radar system. Therefore, noting that, in Equation 8.1, the value of C needs to be minimised in order to maximise the value of total coverage area. Noting that, in Figure 8.1, two ovals intersects at two points, E and F, also can be shown in Figure 8.2. Hence, the coordinates of these two points need to be found in order to obtain an expression for the area of in-

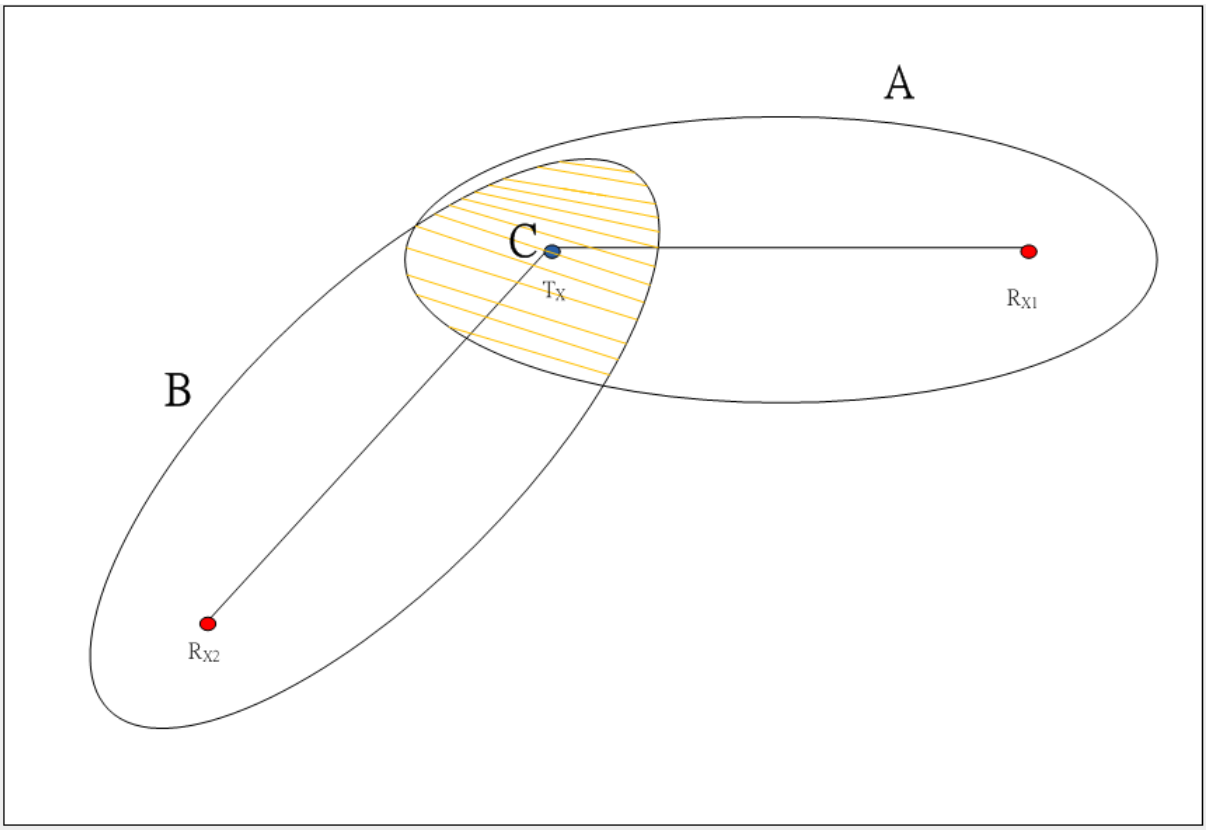

Figure 8.1: Diagram for a standard one transmitter & two receivers passive radar system

tersection. Noting the fact that, both ovals can be expressed in polar coordinates (r,θ) with its origin lying on the mid-point of each baseline which is shown in Equation 2.9. For a better investigation, it will be easier if both origin of axes can be shifted to the point where the transmitter located, as the transmitter is located within the area of intersection and it is the essential link between two ovals. An investigation has been carried out by mathematical calculation to minimise the intersection area of two ovals, as shown in the following chapters.

8.2 Linear Transformation

As shown in Figure 8.2, (r,θ) represents the coordinate for the original axis $(x\&y)$ which has the origin lies on the mid-point of baseline. (r',θ') represents the coordinate for the new axis $(x'\&y')$which the origin lies on the transmitter location. Graphically, this means the original red axis has to be shifted to the position of the green axis as shown in Figure 8.2. The detailed mathematical calculation will be shown below:

From Figure 8.2, noting that,

$$\left(\left(\cos\theta'\right)r' - \frac{1}{2}L_1\right)^2 + \left(\left(\sin\theta'\right)r'\right)^2 = r_1^2$$

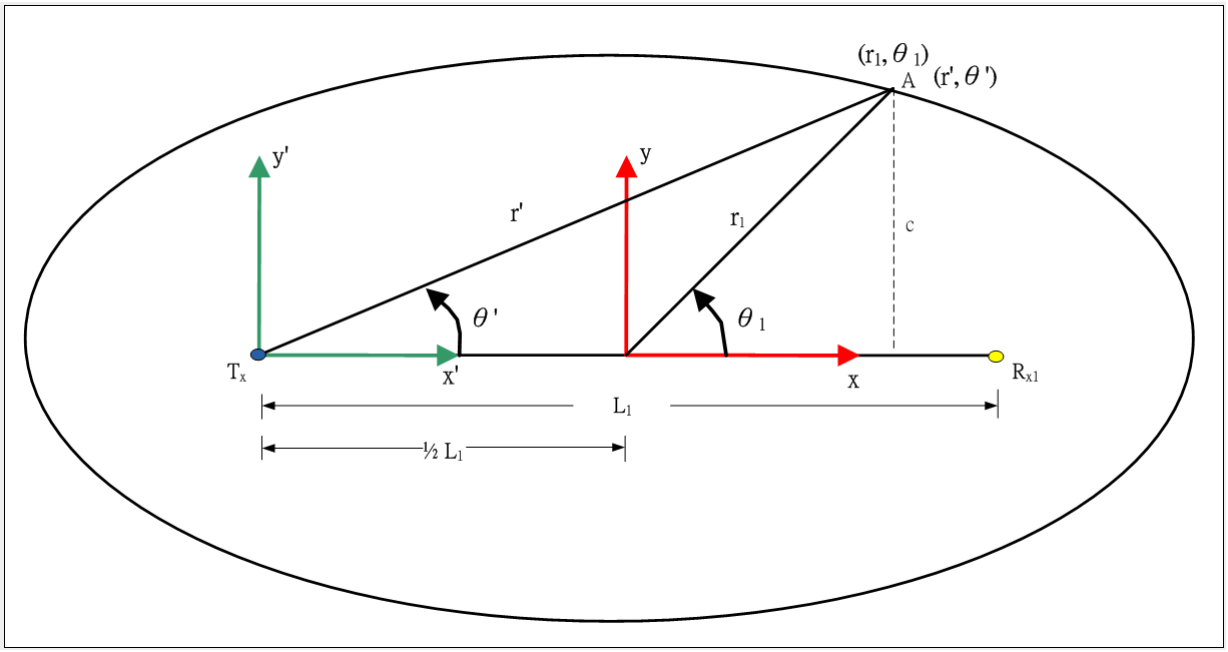

Figure 8.2: Diagram for the illustration of linear transformation

$$\left((\cos\theta)\,r+\frac{1}{2}L_1\right)^2+((\sin\theta)\,r)^2=\left(r'\right)^2$$

and

$$(\sin\theta_1)\,r_1=\left(\sin\theta'\right)r' \tag{8.2}$$

Solving the above two equations, $r_1$and θ_1 can be expressed in the terms of r' and θ'.

$$r_1=f\left(r',\theta'\right)=\sqrt{r'^2-r'L_1\cos\theta'+\frac{1}{4}L_1^2}$$

$$\theta_1=f\left(r',\theta'\right)=\sin^{-1}\left(\frac{r'\sin\theta'}{\sqrt{r'^2-r'L_1\cos\theta'+\frac{1}{4}L_1^2}}\right)$$

In addition, r' and θ' in terms of r_1 and $\theta_1$can also be obtained.

$$r'=f\left(r_1,\theta_1\right)=\sqrt{r_1^2+r_1L_1\cos\theta_1+\frac{1}{4}L_1^2} \tag{8.3}$$

$$\theta' = f(r_1, \theta_1) = \sin^{-1}\left(\frac{r_1 \sin\theta_1}{\sqrt{r_1^2 + r_1 L_1 \cos\theta_1 + \frac{1}{4}L_1^2}}\right) \tag{8.4}$$

A Matlab script called transformation.m has been created to check and ensure the equations that have been obtain shown above are correct. The description of this script will be shown in the Appendix A.

8.3 Linear Transformation with Rotation

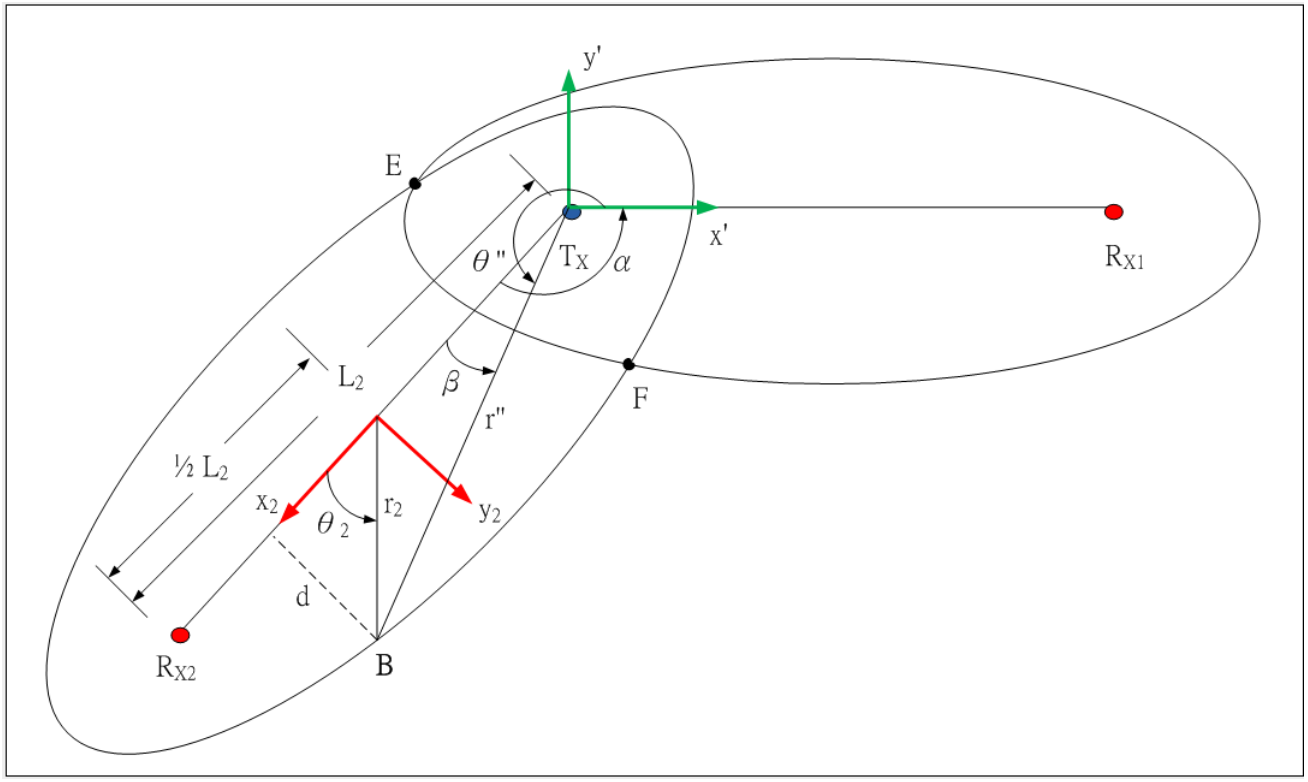

Figure 8.3: Diagram for the illustration of linear transformation with rotation

Figure 8.3 shows the oval of Cassini diagram for the T_X and R_{X2} system. α is the angle between baselines L_1 and L_2. Axis $(x_2 \& y_2)$is the original axis for this oval, and axis $(x' \& y')$ is the new axis which is the same axis as shown in Figure 8.2. The anti-clockwise direction is assumed to be the positive direction, hence, the coordinate of point B with respect to the axis $(x' \& y')$is $(r", \theta")$. Noting that, $\beta = \theta" + \alpha - 2\pi$. Applying the same method that was used in previous paragraph, the following expressions can be yielded.

$r_2$and θ_2 can be expressed in the terms of r" and θ":

$$r_2 = f(r'', \theta'') = \sqrt{r''^2 - r''L_2 \cos(\theta'' + \alpha - 2\pi) + \frac{1}{4}L_2^2}$$

$$\theta_2 = f(r'', \theta'') = \sin^{-1}\left(\frac{r'' \sin(\theta'' + \alpha - 2\pi)}{\sqrt{r''^2 - r''L_2 \cos(\theta'' + \alpha - 2\pi) + \frac{1}{4}L_2^2}}\right)$$

In addition, r'' and θ'' in terms of r_2 and $\theta_2$can also be obtained.

$$r'' = f(r_2, \theta_2) = \sqrt{r_2^2 + r_2 L_2 \cos\theta_2 + \frac{1}{4}L_2^2} \tag{8.5}$$

$$\theta'' = 2\pi + \beta - \alpha = 2\pi + \sin^{-1}\left(\frac{r_2 \sin\theta_2}{\sqrt{r_2^2 + r_2 L_2 \cos\theta_2 + \frac{1}{4}L_2^2}}\right) - \alpha \tag{8.6}$$

Also, a Matlab script called Rotation.m has been created to check and ensure the equations that have been obtain shown above are correct. The description of this script will be shown in the Appendix A.

As shown in Figure 8.3, intersecting points of two oval, point E and F, their coordinates with respect to the oval contains R_{x1}will be the same as the coordinates with respect to the oval contains R_{x2}which all corresponding to the axis located on the transmitter position. This simply means that at point E and F, they both has $r' = r''$and $\theta' = \theta''$. Therefore, intersecting points, E and F, can be solved by equating Equation 8.3 and 8.5, and Equation 8.4 and 8.6. The following equations can be obtained:

$$\sqrt{r_1^2 + r_1 L_1 \cos\theta_1 + \frac{1}{4}L_1^2} = \sqrt{r_2^2 + r_2 L_2 \cos\theta_2 + \frac{1}{4}L_2^2}$$

and

$$\sin^{-1}\left(\frac{r_1 \sin\theta_1}{\sqrt{r_1^2 + r_1 L_1 \cos\theta_1 + \frac{1}{4}L_1^2}}\right) = 2\pi + \sin^{-1}\left(\frac{r_2 \sin\theta_2}{\sqrt{r_2^2 + r_2 L_2 \cos\theta_2 + \frac{1}{4}L_2^2}}\right) - \alpha$$

However, it is very difficult to solve the above equations mathematically due to their non-linearity. The area of intersection will, therefore, be simulated with Matlab based on the expressions shown in above.

8.4 Simulation of Area of Intersection for Two Ovals with Matlab

Firstly, for avoiding complexity, the following assumption has been made in this one transmitter and two receivers system:

$$L_1 = L_2 = L$$

Recording the polar coordinate Equation 5.2 shown in Chapter 5.1, the radius from the origin to the point on the curve (r) can be expressed in terms of the angle (θ) in a oval of Cassini. The expression is shown as following:

$$r = \sqrt{\frac{-\left(\frac{1}{2}L^2 - L^2\cos^2\theta\right) + \sqrt{\left(\frac{1}{2}L^2 - L^2\cos^2\theta\right)^2 - 4\left(\frac{L^4}{16} - \frac{K}{S/N}\right)}}{2}} \tag{8.7}$$

By substituting Equation 8.7 into Equation 8.3 and 8.4 separately, the $r'$and θ'in terms of θ only, can be obtained. r"and θ" in terms of θ only can also be obtained by substituting Equation 8.7 into Equation 8.5 and 8.6 separately. θ has been set to be a matrix contains phase from 0 to $2\pi$with step of 1 degree. Therefore, r' and θ', r"and θ", can be plotted in polar coordinate with the transmitter located at the origin. α is needed to be specified in order to simulate and plot the area of intersection for two ovals. So, α will be set to be 120 degrees ($\frac{2}{3}\pi$ in radian). Hence, Figure 8.4 has been created by using Matlab script called OvalPlot_transfo_coordinate.m.

The position of the point of intersection for two ovals can be measured directly from the simulated plot in Matlab. After obtaining position of these two intersecting points, the two curves that enclose the area of intersection have been given. The value of the area of intersection can then be found by integrating each cell area within the intersected area in the Cartesian grid. However, these tasks have not been carried out in detail due to the time constrain of this project.

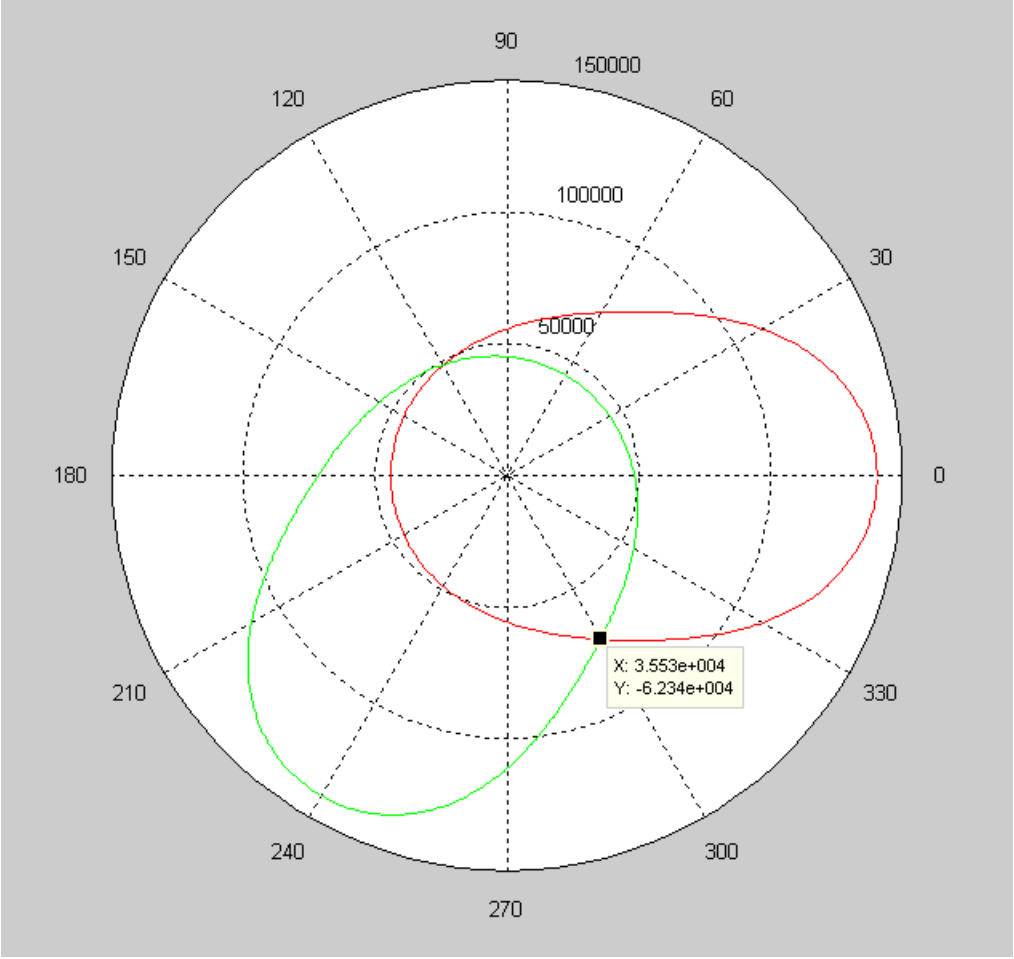

Figure 8.4: Plot of the area of intersection for two ovals of Cassini

Chapter 9

Conclusions and Future Work

This project report focuses on the optimisation of the location of receiver site by investigating the coverage for a passive radar system. A method of maximising the coverage for an one transmitter and one receiver case of passive radar system has been obtained during the investigation. A suggestion on achieving maximum coverage for an one transmitter and two receivers case of passive radar has also been provided.

The establishment of a firm literary base was believed important. Thus to this end, a great deal of literature was studied and reviewed, this review of literature is ultimately presented in Chapter 2 of this project report.

The actual analytical work done in this project report began by setting a criterion for the investigated passive radar system. Thereafter, the relationship between SNR, baseline and coverage area has been investigate. The fact that, for a specific SNR, coverage area in a given one transmitter and one receiver passive radar system only depends on the length of baseline (L). The longer the distance between the transmitter and receiver, the less coverage area will be.

A comparison between the theoretical prediction and the simulated prediction without antenna gain involved in free space has been made. The effects of the antenna gain, multipath, terrain and change in altitude on the coverage area have also been discussed. This is followed by investigating the coverage area in an one transmitter and two receivers passive radar system mathematically. A suggestion has been provided to maximise the coverage area for this case.

In terms of future work, much additional analytical work can be done to further the investigations begun in this project report. In particular, the investigations done in Chapter 8 can be furthered by integrating the area of two enclosed curves from two ovals, hence, to minimise the area of intersection in order to maximise the total coverage area. Due to the limitation of the equipment, all the work done in this project report was in pure theoretical and simulated nature, therefore, all the investigations and analyses carried out here could be verified by practical experiment. In the future, the final goal of this topic is the optimum receiver site can be found automatically in any passive radar system by doing simulation with the realistic data involved.

Appendix A

Matlab Code Description

The Matlab scripts written for this thesis can be found on the CD provided. This appendix lists all the m.files used in this project and gives brief description for each m.file.

Area_vs_Baseline_Plot.m

This stand alone Matlab script will plot the relationship between the coverage and baseline based on the theoretical equation of passive radar area coverage.

FSArea.m

This function will take the SNR data that is generated from AREPS and Multistatic Radar Coverage Prediction Method, then it will count the total number of the desired SNR contained in the SNR data. Therefore, approximated area for the desired SNR can be obtain by multiplying this total number with the area of each cell in the Cartesian grid.

gain_vs_phase_plot.m

This script will plot the antenna gain pattern of the receiver in our practical radar system.

OvalPlot.m

The theoretical oval of Cassini plot for a desired SNR can be obtained by using this Matlab script.

OvalPlot_AREPS.m

This function will take the SNR data produced from the MRCPM, plot the SNR coverage map for the particular passive radar system firstly; Secondly, it will make all the SNR values that bigger than 15dB to be 1 and 0 otherwise. So, a desired SNR coverage area will also be plotted in this Matlab function.

OvalPlot_transfo_coordinate.m

This Matlab script is used to simulate and plot the area of intersection of two ovals based on the equations shown in Chapter 8. Therefore, the coordinates of the points of intersection for two ovals can be obtained. In addition, the plot is plotted with the transmitter sits at the origin of the plot.

Rotation.m

This script is used to verify the equations that obtained from the mathematical prospective shown in Chapter 8. As the fact that the position of the transmitter is given, this script will take a point on the curve of the oval, (r, θ), and use the chosen point to obtain the distance and angle from the transmitter to the point, r' and θ', with irrespectively. By substituting r' and θ' value into the equation for r and θ which are in terms of r' and θ' in order to obtain the theoretical r and θ value. By comparing the theoretical r and $\theta$with the coordinate of the chosen point. If they are identical, it proves that the mathematical prediction is correct.

transformation.m

This script uses the same method shown in Rotation.m to verify the expression for the linear transformation with rotation involved.

Appendix B

CD

This project report comes with a CD containing:

- All Matlab scripts discussed in this project report.
- A PDF version of this project report.

Bibliography

[1] *User's Manual (UM) for Advanced Refractive Effects Prediction System*. Atmospheric Propagation Branch, Space and Naval Warfare System Centre, San Diego, CA, 3.6 edition edition, December 2006.

[2] Atmospheric Propagation Branch. Software programs - introduction of areps. October 2008. URL `http://areps.spawar.navy.mil/`.

[3] James and James. Mathematics dictionary. *Van Nostrand, New York*, 1949.

[4] Gunther Lange. Multistatic radar coverage prediction method. August 2008.

[5] R.J. Lefevre. Bistatic radar: New application for an old technique. In *WESCON Conf. Record, San Francisco*, pages 1–20, 1979.

[6] Christopher L. Zoeller; Dr Mervin C. Budge; Jr. Michael J. Moody. Passive coherent location radar demonstration. 2002.

[7] Hovanessian SA. *Radar System Design and Analysis*. Artech House, January 1984.

[8] Merrill I. Skolnik. *Introduction to Radar Systems 3rd ed*. McGraw-Hill, 2001.

[9] Wikipedia. the free encyclopedia - bistatic radar. October 2008. URL `http://en.wikipedia.org/wiki/Bistatic_radar`.

[10] Wikipedia. the free encyclopedia - passive radar. October 2008. URL `http://en.wikipedia.org/wiki/Passive_radar`.

[11] Nicholas J. Willis. *Bistatic Radar*. SciTech Publishing, Inc., 2005.